POLY(ALLYLAMINE) AND DERIVATIVES FOR CO_2 CAPTURE FROM FLUE GAS OR ULTRA-DILUTE GAS STREAMS SUCH AS AMBIENT AIR

A Thesis
Presented to
The Academic Faculty

by

Ratayakorn Khunsupat

In Partial Fulfillment
of the Requirements for the Degree
Master of Science in the
School of Chemistry and Biochemistry

Georgia Institute of Technology
August 2011

POLY(ALLYLAMINE) AND DERIVATIVES FOR CO_2 CAPTURE FROM FLUE GAS OR ULTRA-DILUTE GAS STREAMS SUCH AS AMBIENT AIR

Approved by:

Dr. Christopher W. Jones, Advisor
School of Chemical & Biomolecular Engineering
Georgia Institute of Technology

Dr. Charles Liotta
School of Chemistry and Biochemistry
Georgia Institute of Technology

Dr. David Collard
School of Chemistry and Biochemistry
Georgia Institute of Technology

Date Approved: June 27, 2011

ACKNOWLEDGEMENTS

This work could not have been completed without the help of many individuals. I would love to start by thanking my advisor, Professor Christopher W. Jones. Thank you very much for giving me the opportunity to develop myself as a chemist who strives for excellence. Dr. Jones provided valuable guidance and helped me build the necessary confidence to challenge myself during the research process. I have really appreciated and enjoyed working with him. I also thank my committee members, Dr. Charles Liotta and Dr. David Collard for their support.

I also thank previous and current members of the Jones group. I would like to thank Dr. Nicholas Brunelli, Dr. Krishnan Venkatasubbaiah, Dr. Mariefel Olarte, Dr. Watcharop Chaikittisilp, Praveen Bollini, Stephanie Didas, Wei Long, Linda Al-Hmoud for all of their advice and encouragement. Without their guidance, I would not have accomplished many of my goals.

Most importantly, I would like to thank my parents, Uthai and Thanyakarn Khunsupat, for all of their unconditional love and support. Without them, I could not have accomplished all that I have.

TABLE OF CONTENTS

LIST OF TABLES

LIST OF FIGURES

LIST OF ABBREVIATIONS

ACPA	4,4-azo-bis(4-cyanopentanoic acid)
AIBN	2,2-azobisisobutyronitrile
APH	2,2-azo-bis-(2-amidinopropane) hydrochloride
Ar	Argon
BET	Brunauer–Emmett–Teller
CO_2	carbon dioxide
Da	Dalton
DVB	divinyl benzene
EPI	epichlorohydrin
EtOH	ethanol
GPC	gel permeation chromatography
HAS	hyperbranched aminosilica
HCl	hydrochloric acid
IPA	isopropanol
MAIB	2,2-azobisiobutyric acid dimethyl ester
MCF	mesocellular foam silica
MeOH	methanol
M_n	number average molecular weight
M_w	weight average molecular weight
NaOH	sodium hydroxide
NH_4F	ammonium fluoride
NMR	nuclear magnetic resonance

PAA	Poly(allylamine)
PAM	Poly(acrylamide)
PDI	poly dispersity index
PEI	Poly(ethylenimine)
PNVF	Poly (*N*-vinyl formamide)
ppm	parts per million
PVAm	Poly(vinylamine)
TGA	thermogravimetric analysis
TOES	tetraethyl orthosilicate

SUMMARY

Polymers rich in primary amine groups are proposed to be effective adsorbents for the reversible adsorption of CO_2 from moderately dilute gas streams (10% CO_2) and ultra-dilute gas streams (e.g. ambient air, 400 ppm CO_2), with their performance under ultra-dilute conditions being competitive with or exceeding the state-of-the-art adsorbents based on supported poly(ethyleneimine) (PEI). The CO_2 adsorption capacity (mmol CO_2/g sorbent) and amine efficiency (mmol CO_2/mmol amine) of linear poly(allylamine) (PAA), cross-linked poly(allylamine) prepared by post-polymerization crosslinking with epichlorohydrin (PAAEPI), and branched poly(allylamine) prepared by branching of poly(allylamine) with divinylbenzene (PAADVB) are presented here and compared with state-of-the-art adsorbents based on supported PEI, specifically branched and linear, low molecular weight PEI.

Silica mesocellular foam, MCF, serves as the support material for impregnation of the amine polymers. In general, branched polymers are found to yield more effective adsorbents materials. Overall, the results of this work show that linear PAA, cross-linked PAAEPI, and branched PAADVB are promising candidates for solid adsorbents with high capacity for CO_2.

CHAPTER 1

INTRODUCTION

Carbon dioxide (CO_2) is one of the greenhouse gases that is suggested to contribute to global climate change. Since the 1750s, there has been an increase of the atmospheric concentration of CO_2 from 277ppm to 377 ppm[1] and it is expected to double by 2050 if the increase continues along the same trend.[2] The main source of increased concentration of atmospheric CO_2 is the emissions from burning fossil fuels, such as natural gas, coal and petroleum for the production of electricity and for transportation. The greatest portion of emissions to the environment is from flue gas released from electricity-generating power plants.[3-5] Consequently, it is important to reduce the rate of increase of the concentration of CO_2 in the atmosphere by reducing emissions from flue gas.

CO_2 can be captured from flue gas (post-decarbonization),[6] separated from synthesis gas, coal/biomass gasification gas, and reformate gas (pre-decarbonization),[7] or even captured from the ambient air (air-decarbonization).[8,9] Regarding these issues, extensive efforts have been devoted to the development of technologies for efficient capture and sequestration of CO_2. Currently, large-scale separation of CO_2 from gas streams by liquid phase amine-based absorption is in commercial operation throughout the world in natural gas separations (purification of methane deposits).[10] The technology also represents the benchmark methodology for CO_2 capture from flue gas (post-combustion CO_2 capture).[11-12] Even though it is the current technology of choice for capturing CO_2, absorption processes still have major drawbacks such as the corrosive properties of liquid amines (e.g. monoethanoamine), the amine loss that occurs during

operation due to amine volatility, solvent degradation in the presence of oxygen and the significant energy consumption in the amine regeneration process, whereby CO_2 is stripped off the amines for concentration and storage.[13] As an alternative to liquid adsorption, the use of solid adsorbents for the separation of CO_2 has several potential advantages. Adsorption on solids does not produce significant wastewater, the adsorbents may be more stable over multiple cycles than liquid amines due to lack of volatility and in some cases, the adsorbent regeneration energies can be lower. Furthermore, if supported amine materials are used, immobilization and confinement of the amine functional groups inside the solid support may produce a stable, mass transfer efficient, less toxic and less corrosive material than liquid amines.

Various porous solid materials have been investigated as CO_2 adsorbents. For instance, physisorbants, which bind CO_2 weakly, such as zeolites 4A, 13X[14-20] and activated carbons[21-23] operate effectively at low temperatures (e.g. room temperature). Because these adsorbents capture CO_2 by physisorption, weak forces are involved (e.g. for zeolites, alkali cation coulombic interactions or for carbons, van der Waals forces) and the heat of adsorption of CO_2 is low.[24-26] This can be advantageous, requiring a low energy for adsorbent regeneration (which is typically achieved via temperature swing with adsorption at low temperature and desorption at high temperature). However, it can also be disadvantageous, as water, which is ubiquitous in flue gases and in ambient air, can out-complete CO_2 for adsorption sites.

To develop a highly efficient adsorbent for CO_2, several research groups have reported excellent performance using mesoporous silica materials incorporating amines. In general, amine groups have been supported on porous solids using three preparation

methods. Class 1 materials are prepared by impregnating a pre-synthesized, amine-containing organic polymer into the pores of the support.[27-29] In this case, the most common polymer used is low molecular weight, highly branched PEI which typically contains primary, secondary and tertiary amines in ratio of roughly 44:33:23[30] or 42:33:25[31], as reported by several authors. Each amine type has potential to bind CO_2 in a classic acid–base interaction. The frequent use of low molecular weight PEI over higher molecular weight polymers is most likely associated with the ease of impregnation into the support pore space because longer polymer chains can sometimes block the pore mouths and prevent complete pore penetration. Class 2 materials are prepared by grafting amine species onto the silica support in a covalent manner. In the grafting approach, amine groups can be efficiently distributed on the surface of the support to exhibit high efficiency for capture of CO_2. However, grafting amines onto solid supports can also be limited by the density of surface grafting sites such as silanol groups on silica materials, which leads to a relatively low CO_2 adsorptive capacity of the resulting composite.[32-35] For these materials, amine loading often scales with the support surface area. In contrast, for class 1 materials, amine loading scales with the support pore volume.

Class 3 materials were invented by our group at Georgia Tech, and are comprised of polymer-silica composite materials prepared by the in-situ polymerization of amine-containing monomers off the silica support. Aziridine is the monomer most commonly used, producing grafted hyperbranched polymers grown off the surface. These materials have been referred to as hyperbranched aminosilica (HAS) materials.[30] A schematic description of all three classes of supported amine adsorbents is presented in Figure 1.1.

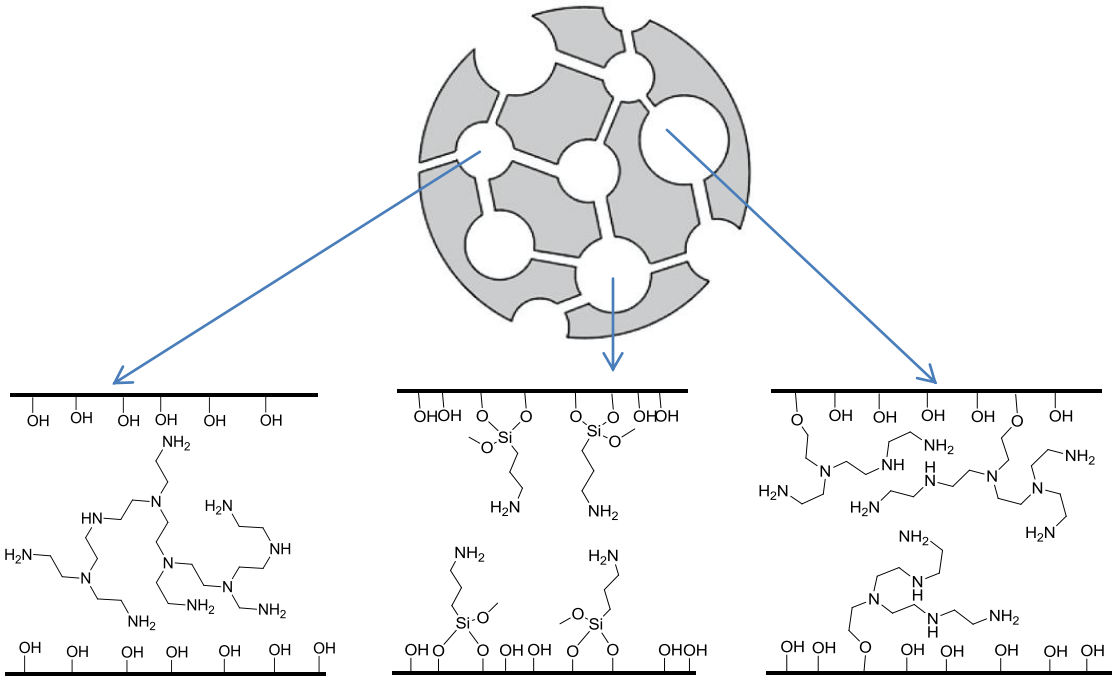

Figure 1.1. Schematic class 1, 2 and 3 of supported amine adsorbents

The reaction of CO_2 with amines in solution has been studied by several groups. Primary and secondary amines react directly with CO_2 to form carbamate ions. The reactions occur via a zwitterionic mechanism, whereby the amine reacts directly with CO_2 to produce carbamates through the formation of zwitterionic intermediates shown in Figure 1.2.[32] The reaction can be described as occurring by the lone pair on the amine acting as a nucleophile or electron donor, attacking the carbon from CO_2 to form the zwitterions, followed by additional free base deprotonating the zwitterion to form the carbamate. Accordingly, under dry conditions where the interaction of CO_2 with amine occurs in a water-free environment, carbamate formation, requires 2 amine groups per CO_2 molecule (i.e., CO_2 /N=0.5). Under humid conditions, where H_2O can acts as a base only one amine group is required per CO_2 molecule. Thus, the CO_2 adsorption capacities

for this condition may be double that of dry case when using primary or secondary amines. The maximum amine efficiency of an amine adsorbent in the presence of water is 1.0 mol CO_2 per mol N, since only one mole of amine is required per mole of CO_2 captured (i.e., CO_2 /N=1) but it is only 0.5 mol CO_2 per mol N under dry conditions. The ability to form carbamate ions allows for direct reaction of the amine with CO_2, which generally produces fast CO_2 capture kinetics for primary and secondary amines. In this thesis, I will define amine efficiency as a reflection of the adsorbent's efficacy in perspective with its potential. Amine efficiency, defined here as the number of moles of CO_2 captured per mass unit divided by the moles of N per mass unit.

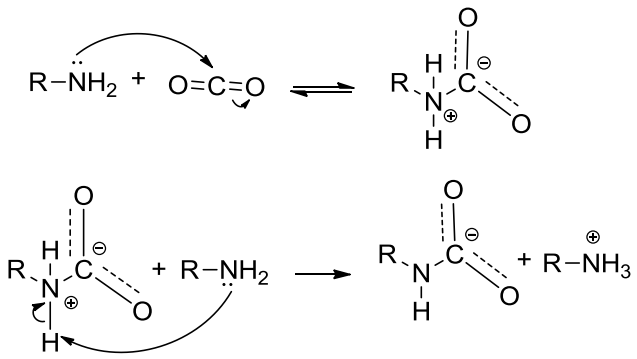

Figure 1.2. Mechanism for cabarmate formation of CO_2 with primary, secondary amines.

Tertiary amines are generally not used for CO_2 capture, because they do not react with CO_2 to produce carbamate ions. Tertiary amines, however, can remove a stoichiometric amount of CO_2 by reaction with water to produce hydroxyl ions that can then react with CO_2 to produce bicarbonate ions. The mechanism of the reaction is shown in Figure 1.3.[33-35] In the first step, the lone pair nucleoplile on the tertiary amine dissociates H_2O to form a quaternary cationic species and hydroxide ion. Hydroxide ion then attacks CO_2 to form the bicarbonate anion. The last step is the ionic association of

the protonated amine and bicarbonate. The kinetics of CO_2 removal by tertiary amines is generally slower than for primary and secondary amines.

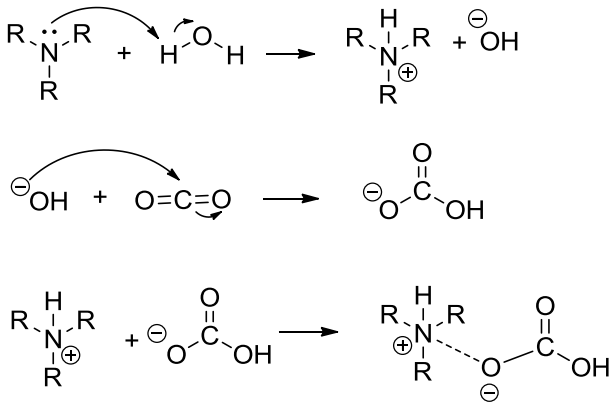

Figure 1.3. Mechanism for the reaction of CO_2 with tertiary amines.

As noted above, one-third of global carbon emissions are associated with distributed sources such as aircraft or automobiles.[3,5] Whereas capture from fixed point sources such as coal-fired power plants is feasible using post-combustion CO_2 capture technologies, addressing the CO_2 release from the mobile sources such as cars and planes is far more difficult. One potential way to address all emission sources, regardless of type, is via the direct extraction of CO_2 from the ambient atmosphere. Lackner et al. first proposed the removal of CO_2 from ambient air for carbon capture and storage in 1999.[36,37] Other researchers have demonstrated methods to extract CO_2 from the ambient air and evaluated the performance of different approaches.[38-43] The challenge in removing CO_2 from ambient air ("air capture") lies in its low concentration. Today, the ambient air concentration is approximately 400 ppm whereas flue gas is 10-20% CO_2 by volume. Thus, CO_2 capture from ambient air requires an extremely efficient adsorbent tuned to bind CO_2 very strongly, and to capture a large quantity of CO_2 massive volumes

of air must be processed. Such a process requires more gas to be moved through a larger adsorber than with conventional flue gas scrubbing.

Various alkali metal oxides or hydroxides are potential candidates for air capture.[42, 44-46] Removal of CO_2 with alkali metal oxides or hydroxides involves a chemical reaction that results in the formation of alkali carbonates or bicarbonates. Regeneration of these materials requires high temperature (900ºC) because it involves the decomposition of the alkali carbonates formed during adsorption. The high regeneration energies of these sorbents results in a significant loss in system efficiency. For a practical air capture design, an approach that requires relatively low regeneration energy is needed, and ideally the process will operate near ambient conditions.

Using solid adsorbents for air capture has been investigated in several research groups.[43,47,48] The array of classical CO_2 adsorbents has been primarily evaluated for CO_2 capture from flue gas,[25] as mentioned above. However, the strict requirements of air capture substantially limit this list of potential adsorbents for air capture applications. For example, physisorbents that absorb CO_2 via weak physical interactions such as zeolites and activated carbons have low CO_2 adsorption capacities in air capture because the heat of adsorption is low, leading to shallow adsorption isotherms with low adsorption capacities at low partial pressures (Figure 1.4).[49]

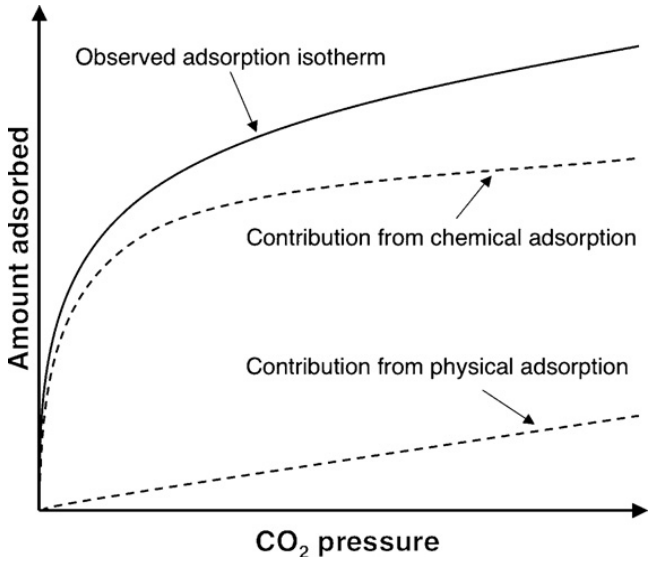

Figure 1.4. Schematic representation of CO_2 adsorption on amine-functionalized mesoporous adsorbents. [49]

As the concentration of CO_2 in ambient air is extremely dilute, about 400 ppm, a potentially useful adsorbent for air capture would have a relatively high heat of adsorption yielding a steep adsorption isotherm with high adsorption capacities at ultra low partial pressures. Solid amine-functionalized materials based on primary, secondary or tertiary amines operate near ambient conditions, are tolerant to water vapor, and they can be regenerated by mild temperature swings.[25] It is known that primary amines have higher heats of adsorption than that of secondary and tertiary amines.[50,51] This thesis hypothesize that supported amine adsorbents based on polymers containing only or mostly primary amines sites will therefore be promising adsorbents for CO_2 capture from ultra-dilute gas streams, such as ambient air. Furthermore such materials should also offer performance comparable to other supported amine adsorbents at moderate gas pressures found in typical post-combustion capture processes targeting flue gases from large point sources such as coal-fired power plants.

In the last three years, our group has demonstrated that supported amine materials efficiently extract CO_2 from simulated ambient air.[9] Specifically, the group has demonstrated that PEI-based class 1[52] and class 3[43] supported amine adsorbents effectively extract CO_2 from simulated ambient air more efficiently than class 2 sorbents described by others.[53] Thus, class 1, PEI-based sorbents are the current benchmark sorbents for CO_2 capture from ambient air. However, as noted above, PEI contains a distribution of primary, secondary and tertiary amines sites, and we hypothesize that only primary amines are responsible for adsorption from gases with ambient air concentrations (400 ppm). The major goals of this thesis are (1) to synthesize and characterize polymers that are rich in primary amines. (2) create class 1 adsorbents using these polymers, by impregnating the polymers into the pore space of a large pore mesocellular foam silica, and (3) to evaluate the CO_2 adsorption capacities of the new polymeric amine–silica composite materials under simulated air capture and flue gas capture conditions and (4) to assess the impact of polymer cross-linking and branching on the CO_2 adsorption properties.

References

1. Marland, G.;Boden, T.A., Andres, R.J. Global, Rigional, and National Fossil Fuels CO_2 Emissions. Trends: A Compendium of Data on Global Change, Oak Ridge, TN: Oak Ridge National Laboratory **2007**, http://cdiac.ornl.gov/trends/emis/tre_glob.htm.

2. Nielsen, R. Nuclear Power Plants 2007, http://home.iprimus.com.au/nielsens/nuclear.html.

3. Benson, S.; Abanades,J.C.; Akai, M.; *IPCC Special Report Carbon Dioxide Capture Storage* 2005, http://www.ipcc.ch/pdf/special-reports/srccs/srccs_summaryforpolicymakers.pdf.

4. Pacala, S.; Socolow, R. Stabilization Wedges: Solving the Climate Problem for the Next 50 Years with Current Technologies. *Science* **2004**, 305, 968.

5. EIA. Annual Energy Outlook **2007**, Table A18 www.eia.doe.gov.

6. Services, R.F. The Carbon Conundrum. *Science* **2004**, 305, 962.

7. Kintisch, E. The Greening of Synfuels. *Science* **2008**, 320, 306.

8. Stolaroff, J.K.; Keith, D.W.; Lowry, G.V. Carbon Dioxide Capture from Atmospheric Air Using Sodium Hydroxide Spray, *Environ. Sci. Technol* **2008**, 42, 2728.

9. Choi, S. D., J. H.; Eisenberger, P. M.; Jones, C. W. In *AIChE Annual Meeting* Nashville, TN, 2009.

10. http://www.naturalgas.org/naturalgas/processing_ng.asp

11. Hammond, G. P.; Akwe, S. S. O. Thermodynamic and related analysis of natural gas combined cycle power plant with and without carbon sequestration, *Int. J. Energy Res.* **2007**, *31*, 1180.

12. Tobiesen, F. A.; Svendsen, H. F.; Mejdell, T. Modeling of Blast Furnace CO_2 Capture Using Amine Absorbents, *Ind. Eng. Chem. Res.* **2007**, *46*, 7811.

13. Veawab, A.; Tontiwachwuthikul, P.; Chakma, A. Corrosion Behavior of Carbon Steel in the CO_2 Absorption Process Using Aqueous Amine Solutions, *Ind. Eng. Chem. Res.* **1999**, 38, 3917.

14. Takamura, Y.; Narita, S.; Aoki, J.; Hironaka, S.; Uchida, S. Evaluation of dual-bed pressure swing adsorption for CO_2 recovery from boiler exhaust gas. *Sep. Purif. Technol*. **2001**, 24, 519.

15. Reynolds, S.P.; Ebner, A.D.; Ritter, J.A. Carbon dioxide capture from flue gas by pressure swing adsorption at high temperature using a K-promoted HTlc: effects of mass transfer on the process performance. *Environ. Prog*. **2006**, 25, 334.

16. Gomes, V.G.; Yee, W.K. Pressure swing adsorption for carbon dioxide sequestration from exhaust gases. *Sep. Purif. Technol*. **2002**, 28, 161.

17. Merel, J.; Clausse, M.; Meunier, F. Carbon dioxide capture by indirect thermal swing adsorption using 13X zeolite. *Environ. Prog.* **2006**, 25, 327.

18. Sebastian, V.; Kumakiri, I.; Bredesen, R.; Menendez, M. Zeolite membrane for CO_2 removal: operating at high pressure, *J. Membr. Sci.* **2007,** 292, 92.

19. Calleja, G.; Jimenez, A.; Pau, J.; Dominguez, L.; Pbrez, P. Multicomponent adsorption equilibrium of ethylene, propane, propylene and CO_2 on 13X zeolite. *Gas Sep. Purif.* **1994**, 8, 247.

20. Walton, K.S.; Abney, M.B.; Levan, M.D. CO_2 adsorption in Y and X zeolites modified by alkali metal cation exchange, *Micro. Meso. Mater*. **2006**, 91, 78.

21. Siriwardane, R.V.; Shen, M.S.; Fisher, E.P.; Poston, J.A. Adsorption of CO_2 on molecular sieves and activated carbon. *Energy Fuels* **2001**, 15, 279.

22. Na, B.K.; Koo, K.K.; Eum, H.M.; Lee, H.; Song, H.K. CO_2 recovery from flue gas by PSA process using activated carbon. *Korean J. Chem. Eng*. **2001**, 18, 220.

23. Chen, J.H.; Wong, D.S.H.; Tan, C.S. Adsorption and desorption of carbon dioxide onto and from activated carbon at high pressures. *Ind. Eng. Chem. Res.***1997**, 36, 2808.

24. Chue, K. T.; Kim, J. N.; Yoo, Y. J.; Cho, S. H. Comparison of Activated Carbon and Zeolite 13X for CO_2 Recovery from Flue Gas by Pressure Swing Adsorption. *Ind. Eng. Chem. Res.* **1995**, *34*, 591.

25. Choi, S.; Drese, J. H.; Jones, C. W. Adsorbent materials for carbon dioxide capture from large anthropogenic point sources. *ChemSusChem* **2009**, 2, 796.

26. Rege, S. U.; Yang, R. T.; Buzanowski, M. A. Sorbents for air prepurification in air separation. *Chem. Eng. Sci*. **2000**, 55, 4827.

27. Xu, X. C.; Song, C. S.; Andresen, J. M.; Miller, B. G.; Scaroni, A. W. Novel polyethylenimine-modified mesoporous molecular sieve of MCM-41 type as high-capacity adsorbent for CO_2 capture. *Energy Fuels* **2002**, 16, 1463.

28. Xu, X. C.; Song, C. S.; Andresen, J. M.; Miller, B. G.; Scaroni, A. W. Preparation and characterization of novel CO2 "molecular basket" adsorbents based on polymer-modified mesoporous molecular sieve MCM-41. *Micro. Meso. Mater.* **2003**, 62, 29.

29. Xu, X. C.; Song, C. S.; Miller, B. G.; Scaroni, A. W. Adsorption separation of carbon dioxide from flue gas of natural gas-fired boiler by a novel nanoporous "molecular basket" adsorbent. *Fuel Processing Technol*. **2005**, 86, 1457.

30. Hicks, J.C.; Dress, J.H.; Fauth, D.J.; Gray, M.L.; Qi, G.G.; Jones, C.W. Designing Adsorbents for CO_2 Capture from Flue Gas-Hyperbranched Aminosilicas Capable of Capturing CO_2 Reversibly. *J. Am. Chem. Soc*. **2008**, 130, 2902.

31. von Harpe,A.; Petersen, H.; Li, Y.; Kissel, T. Characterization of commercially available and synthesized polyethylenimines for gene delivery. *J. Controlled Release* **2000**, 69, 309.

32. Diaf,A.; Garcia, J.L., Beckman, E.J. Thermally reversible polymeric sorbents for acid gases: CO_2, SO_2, and NOx. *J. Appl. Polym. Sci*. **1994**, 53, 857.

33. Harlick, P. J. E.; Sayari, A. Applications of pore-expanded mesoporous silica. 5. Triamine grafted material with exceptional CO_2 dynamic and equilibrium adsorption performance. *Ind. Eng. Chem. Res*.**2007**, 46 (2), 446.

34. Khatri, R. A.; Chuang, S. S. C.; Soong, Y.; Gray, M. Carbon dioxide capture by diamine-grafted SBA-15: A combined Fourier transform infrared and mass spectrometry study. *Ind. Eng. Chem. Res*. **2005**, 44 (10), 3702.

35. Tsuda, T.; Fujiwara, T.; Taketani, Y.; Saegusa, T. Amino silicagels acting as a carbon dioxide absorbent. *Chem. Lett*. **1992**, 11, 2161.

36. Lackner, K. S.; Ziock, H.; Grimes, P., Carbon dioxide extraction from air: Is it an option? The 24th International Conference on Coal Utilization & Fuel Systems, Clearwater, FL, 1999.

37. Lackner, K. S.; Grimes, P.; Ziock, H. Carbon dioxide extraction from air? Los Alamos National Laboratory, LAUR-99-5113, Los Alamos, NM, 1999.

38. Nikulshina, V.; Ayesa, N.; Galvez, M. E.; Steinfeld, A. Feasibility of Na-based thermochemical cycles for the capture of CO_2 from air -Thermodynamic and thermogravimetric analyses. *Chem. Eng. J*. **2008**, 140 (1-3), 62–70.

39. Keith, D. W. Why capture CO_2 from the atmosphere? *Science* **2009**, 325 (5948), 1654.

40. Baciocchi, R.; Storti, G.; Mazzotti, M. Process design and energy requirements for the capture of carbon dioxide from air. *Chem. Eng. Process*. **2006**, 45 (12), 1047.

41. Stolaroff, J. K.; Keith, D. W.; Lowry, G. V. Carbon dioxide capture from atmospheric air using sodium hydroxide spray. *Environ. Sci. Technol.* **2008**, 42 (8), 2728.

42. Zeman, F. Energy and material balance of CO_2 capture from ambient air. *Environ. Sci. Technol*. **2007**, 41 (21), 7558.

43. Choi, S.; Drese, J.H.; Eisenberger, P.M.; Jones, C.W. Application of Amine-Tethered Solid Sorbents for Direct CO_2 Capture from the Ambient Air. *Environ. Sci. Technol*. **2011**, 45, 2420.

44. Mahmoudkhani, M.; Keith, D. W. Low-energy sodium hydroxide recovery for CO_2 capture from atmospheric air-Thermodynamic analysis. *Int. J. Greenhouse Gas Control* **2009**, 3 (4), 376.

45. Nikulshina, V.; Gebald, C.; Steinfeld, A. CO_2 capture from atmospheric air via consecutive CaO-carbonation and $CaCO_3$-calcination cycles in a fluidized-bed solar reactor. *Chem. Eng. J.* **2009**, 146 (2), 244.

46. Duan, Y.; Zhang, B.; Sorescu; D.C.; Johnson, J.K. CO_2 capture propertiesof M–C–O–H (M=Li, Na,K)systems:Acombined density functionaltheoryandlatticephonondynamicsstudy. *J. Solid State Chem.* **2011**, 184, 304.

47. Lackner, K. S. Capture of carbon dioxide from ambient air. *Eur. Phys. J. Spec. Top*. **2009**, 176, 93.

48. Belmabkhout, Y.; Serna-Guerrero, R.; Sayari, A. Amine-bearing mesoporous silica for CO_2 removal from dry and humid air. *Chem. Eng. Sci.* **2010**, 65 (11), 3695.

49. Serrna-Guerrero, R.; Belmabkhout, Y.; Sayari, A. Modeling CO_2 adsorption on amine-functionalized mesoporous silica: 1. A semi-empirical equilibrium model. *Chem. Eng. J.* **2010**, 161, 173.

50. Xiaoliang, M.; Chunshan, S. Removal of H_2S and CO_2 from gas mixtures by adsorption on polymer-based adsorbents for hydrogen production: A computational chemistry approach. *Prepr.Pap. – Am. Chem.Soc., Div. Petr.Chem.* **2006**, 51(1), 100.

51. Filburn, T.; Helble, J. J.; Weiss, R. A. Development of Supported Ethanolamines and Modified Ethanolamines for CO_2 Capture. *Ind. Eng. Chem. Res.* **2005**, *44*, 1542.

52. Choi, S.; Gray, M.L.; Jones, C.W. Amine-Tethered Solid Adsorbents Coupling High Adsorption Capacity and Regenerability for CO_2 Capture From Ambient Air. *ChemSusChem*, **2011**, 4, 628.

53. Belmabkhout, Y.; Sayari, A. Adsorption of CO_2 from dry gases on MCM-41 silica at ambient temperature and high pressure. 1: Pure CO_2 adsorption. *Chem. Eng. Sci*. **2009**, 64, 3729.

CHAPTER 2

PRIMARY AMINE-RICH POLYMERS FOR CO_2 CAPTURE FROM FLUE GAS OR ULTRA-DILUTE GAS STREAMS SUCH AS AMBIENT AIR

2.1 Introduction

CO_2 adsorption from ultra-dilute gas streams (<1% CO_2 by volume) such as ambient air (350-450 ppm CO_2 by volume) requires adsorbents tuned to bind CO_2 very strongly.[1] Solid amine-functionalized materials are known to effectively bind CO_2 and extract it from gas streams. One class of adsorbents, deemed class 1 supported amine adsorbents by Jones,[2] composed of polymeric amines impregnated onto a porous support, is well known to be an effective adsorbent for CO_2 capture from moderately dilute flue gas streams (5-20% CO_2 by volume). The most commonly used polymer is poly(ethylenimine) (PEI), which contains a mixture of primary, secondary and tertiary amines.[3-4] It is known that adsorbents with a higher heat of adsorption will have a steeper adsorption isotherm, leading to materials with larger adsorption capacities at low target gas partial pressures.[1, 5-6] It is known that primary amines generally have higher heats of adsorption with CO_2 than secondary and tertiary amines.[7-9] I hypothesize that supported amine adsorbents based on polymers containing only or primarily primary amines sites will therefore be promising adsorbents for CO_2 capture from ultra-dilute gas streams, such as ambient air. Furthermore, it should also offer comparable performance to other supported amine adsorbents at moderate gas pressures found in typical post-combustion capture processes targeting flue gas from large point sources such as coal-fired power plants.

The goals of this chapter are (1) to synthesize and characterize polymers that are rich in primary amines, (2) create class 1 adsorbents using these polymers, by impregnating the polymers into the pore space of a large pore mesocellular foam silica, and (3) to evaluate the CO_2 adsorption capacities of the new polymeric amine – silica composite materials under simulated air capture and flue gas capture conditions.

Poly(vinylamine) (PVAm) and poly(allylamine) (PAA) were chosen as candidate polymers in this research because they both contain primary amines and they have a minimal amount of carbon atoms that add unwanted sensible heat to adsorbents sued in a thermal swing process. To investigate the efficiency of CO_2 capture using these primary amine polymers, it is important to compare their performance with low molecular weight, branched PEI and linear PEI as benchmarks. Low molecular weight (~800 Da) branched PEI is the benchmark polymer that gives the highest CO_2 adsorption capacities. It contains a mixture of primary, secondary and tertiary amines, with the primary amines likely highly accessible, displayed on the chain ends. Linear PEI contains only secondary amines, with the exception of primary amines on each chain end. The structures of PVAm, PAA, PEI branched and PEI linear are presented in Figure 2.1.

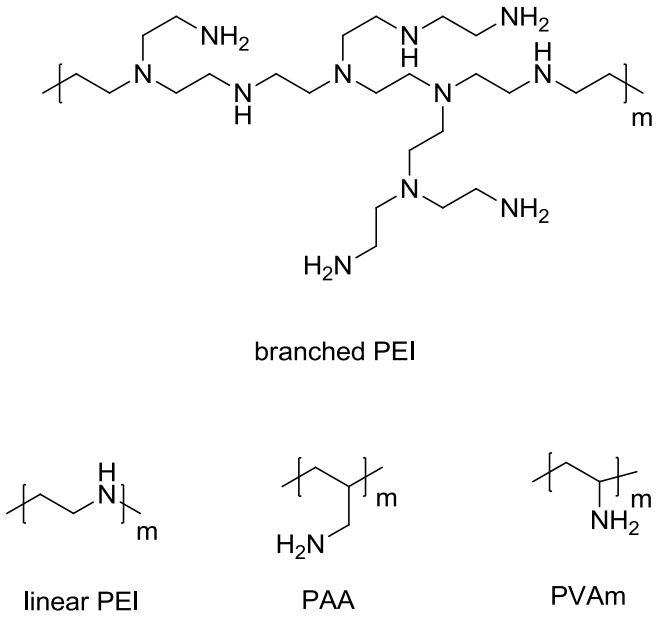

Figure 2.1. Structure of amine polymers

2.2 Experiment

2.2.1 Materials

The following chemicals were used as received from the supplier: Allylamine hydrochloride (AAHCl, TCI), isopropanol anhydrous (IPA, 99.5%, Alfa Aesar), methanol (MeOH, 99.5%, Sigma Aldrich), ethanol (EtOH, 99.5%, ACROS), 2,2-azobisiobutyric acid dimethyl ester (MAIB, 98 %, AK Scientific), 2,2-azobisisobutyronitrile (AIBN, 98%, Sigma-Aldrich), 4,4-azo-bis(4-cyanopentanoic acid) (ACPA,98%, Sigma-Aldrich), 2,2-azo-bis-(2-amidinopropane) hydrochloride (APH, 98%, Sigma-Aldrich), strongly basic ion exchange resin (Ambersep 900 OH^- form, Sigma-Aldrich), poly(acrylamide) GPC standards (PAM2950, PAM15K, PAM100K, American Polymer Standards), water for GPC (TraceSelect, Sigma Aldrich), Pluronic P123 EO-PO-EO triblock copolymer (P123, Sigma-Aldrich), 1,3,5-trimethylbenzene (TMB, 97%,Sigma-Aldrich), tetraethyl orthosilicate (TEOS, 98%,Sigma-Aldrich),

ammonium fluoride (NH_4F, >96%, Alfa Aesar), hydrochloric acid (HCl, conc. 37%, J.T. Baker), branched poly(ethylenimine), M_w 800 Da (branched PEI, Sigma-Aldrich), linear poly(ethylenimine), M_w 2,500 Da (linear PEI, Polyscience).

2.2.2 Synthesis of Polymers

2.2.2.1 Synthesis of Poly(vinylamine), PVAm

2.2.2.1.1 Synthesis of Poly(N-vinylformamide), PNVF

A mixture of *N*-vinylformamide (2.00g, 0.03mol), isopropanol (10mL) and AIBN (0.36mg, 18wt% relative to the monomer) were degassed by three freeze-pump-thaw cycles. The polymerization was carried out in an oil bath at 65°C for 18h under an argon atmosphere. The polymer was precipitated by excess acetone two times to remove unreacted monomer, then dried under vacuum for 24h to give PNVF 1.8g (90%).

2.2.2.1.2 Hydrolysis of PNVF

A solution of PNVF (1.5g in 73.0g of 2*N* NaOH, 2wt% polymer concentration) was degassed by argon purging for 1h. The solution was kept at a constant temperature of 75°C for 64h. After cooling to room temperature, the resulting PVAm polymer was acidified with concentrated HCl to precipitate the PVAm-HCl salt. The precipitate was washed with methanol and dried under vacuum to give 1.3g (90%). ^{1}H NMR (400MHz, D_2O, ppm) 1.57(-CH_2-), 3.79 (-CH-), 7.52-8.07 (HCO-).

PVAm was obtained by using a strongly basic ion exchange resin OH^- form to remove the HCl. Additional degassed deionized water (30mL) and strongly basic ion exchange resin OH^- form (16g) were added to the mixture and stirred for 1h. The solution of PVAm polymer at pH 12 was filtered, the solvents were removed by vacuum

and the residue was dried under vacuum for 24h to give 1.40g product (90%). ^{1}H NMR (400MHz, D_2O, ppm): 2.16 (-CH_2-), 3.74 (-CH-).

2.2.2.2 Synthesis of Poly(allylamine), PAA

The solution of allylamine hydrochloride (6.00g, 0.06mol), isopropanol (3.99g) and MAIB (0.79g, 3.43mmol) was deaerated by argon purging for 1h. The polymerization was carried out at a constant temperature of 60°C for 48h. The resulting polymer was washed with excess methanol to remove unreacted monomer. PAA-HCl was recovered by filtration and dried under vacuum at room temperature for 24h to give 4.5g of white powder (70%). ^{1}H NMR (400MHz, D_2O, ppm): 1.37 (-CH_2-), 1.90 (-CH-), 2.91 (-CH_2-).

PAA was obtained by using a strongly basic ion exchange resin OH^- form to remove the HCl. Additional degassed deionized water (30mL) and strongly basic ion exchange resin (16g) were added to the mixture and stirred for 1h. The resulting polymer solution at pH 12 was filtered, the solvent was removed by vacuum and the polymer dried under vacuum for 24h to give 4.0g of product (60%). ^{1}H NMR (400MHz, D_2O, ppm) 1.14 (-CH_2-), 1.52 (-CH-), 2.59 (-CH_2-).

2.2.3 Synthesis of Silica Mesocellular Foam, MCF

A solution of P123 (16.0g), water (260g) and concentrated HCl (47.4g) were stirred for 24h to complete copolymer dissolution. The flask was then transferred to a 40°C oil bath and TMB (1.6g) was added. The mixture was stirred at 40°C for 2h, then TEOS (34.6g) was added. The solution was stirred an additional 5min and then left quiescent for 20h at 40°C. A solution of NH_4F 184 mg in deionized water (20mL) was added as a mineralization agent and the mixture was swirled for 5 min before aging at

constant temperature of 100°C for 24h. The resulting precipitate was filtered, washed with excess water, dried, and calcined in air at 550°C for 6h (1.2°C/ min ramp). A typical silica MCF was obtained, 15g (95%).

2.2.4 Impregnation of Polymers in MCF

The amine polymer-loaded MCF samples in different weight percentage loadings were prepared by a wet impregnation method. In a typical preparation, the desired amount of amine polymer was dissolved in methanol under stirring for about 15min while purging the mixture with argon gas, until the polymer dissolved completely. Then, the necessary amount of calcined MCF was added to the mixture. The resulting mixture was stirred for 16h under an argon atmosphere. The mass ratio of methanol or ethanol:MCF was always maintained constant at 28:1 for each sample, while the ratio of MCF:polymer was varied in each case. The resulting final solid was recovered by removal of the solvent under vacuum and drying under vacuum at ambient temperature for 24h. The as-prepared adsorbents were denoted as X_MCF_Y, where X represents the amine polymer, Y represents the polymer weight percentage in the sample. Branched PEI, linear PEI, linear PAA are referred to as PEIBR, PEILN, PAALN, respectively. Branched PEI materials were prepared in two samples sets. The as-prepared branched PEI sample sets 1 and 2 were denoted as PEIBR_MCF(1) and PEIBR_MCF(2), respectively.

2.2.5 Characterization

The polymer structure was characterized using solution ^{1}H NMR. The measurements were performed using a Mercury Vx 400 MHz with D_2O as solvent.

Molecular weights of the polymers were determined by gel permeation chromatography, GPC, at 30°C. The GPC system was comprised of a Shimadzu LC-20AD pump, a Shimadzu RID-10A RI detector, a Shimadzu SPD-20A UV detector, a Shimadzu CTO-20A column oven, and Viscotek TSK Viscogel PWXL Guard, G3000, G4000, and G6000 columns mounted in series. The mobile phase consisted of 0.05*N* $NaNO_3$ and the flow rate was maintained at 0.4mL/min. Poly (acrylamide) standards were used (M_w 3350, 15500, 99000), (M_n 2765, 12800, 45600). The surface area, total pore volume and pore size distributions were determined by nitrogen adsorption–desorption isotherm measurements at 77K using a Micromeritics TRISTAR2002. The samples were degassed under vacuum at 100°C overnight before the adsorption measurements. The surface area was determined by the Brunauer–Emmett–Teller (BET) method. Total pore volume, and cell and window pore size were calculated using the Broekhoff-de Boer method with the Frenkel–Halsey–Hill (BdB-FHH) modification.[10] Total pore volume was calculated from the amount of absorbed nitrogen at P/P_o=0.99. The organic loading of the materials was characterized by combustion using a Netzsch STA409 TGA under a flowing nitrogen diluted air stream. About 10 mg of the sample was heated from 27-740°C at a rate of 10°C/min.

2.2.6 CO_2 Adsorption

The CO_2 adsorption characteristics of the amine polymer-loaded MCF materials were characterized using a TA Q500 thermogravimetric analyzer. A sample weight of about 20mg of sorbent was loaded in a platinum vessel and tested for CO_2 adsorption performance. The initial activation of the sample was carried out at 120°C for 3h after heating to that temperature at 5°C/min rate under an Ar flow of a 100ml/min. Then, the

temperature was decreased to 25°C and held for 1h at that temperature before introducing CO_2. Adsorption was then initiated by exposing the samples to the dry target gas of desired concentration (400 ppm CO_2 or 10% CO_2 balanced with Ar) at a flow rate of 100 mL/min. The adsorption experiment was performed until the pseudo-equilibrium capacity was reached, which was determined to be the time when the weight gains from adsorbed CO_2 changed by less than 0.0001 %/min. The adsorption runs were conducted for 12h for 400ppm gas experiments and 3h for 10% CO_2 experiments.

2.3 Results and Discussion

2.3.1 Characterization of synthesized polymers

2.3.1.1 Poly(vinylamine), PVAm

The synthesis of PVAm involved free-radical polymerization of *N*-vinylformamide, to yield poly(*N*-vinylformamide) (PNVF) that was base hydrolyzed to yields PVAm (Figure 2.2).[11] The hydrolysis was carried out under basic conditions, as opposed to acidic conditions, to allow for complete conversion, since there is no positive charge built up on polymer chain during hydrolysis to limit further hydrolysis of the remaining formamide.[12]

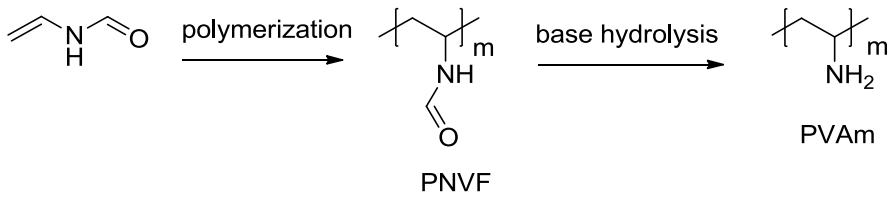

Figure 2.2. Schematic description of the synthesis route of PVAm.

The ^{1}H NMR spectrum (400MHz, D_2O, ppm) 1.57(-CH_2-), 3.79 (-CH-), 7.52-8.07 (HCO-) in Figure 2.3 presents the structure of the parent PNVF, whereas the ^{1}H NMR spectrum (400MHz, D_2O, ppm): 2.16 (-CH_2-), 3.74 (-CH-) in Figure 2.4 described the

resulting PVAm, after hydrolysis. As can be seen, the multiplets at 7.52-8.07 ppm from formamide protons accommodated in chains with diverse polymer tacticity in PNVF disappeared after the base hydrolysis, indicating that the PVAm was successfully synthesized.[13]

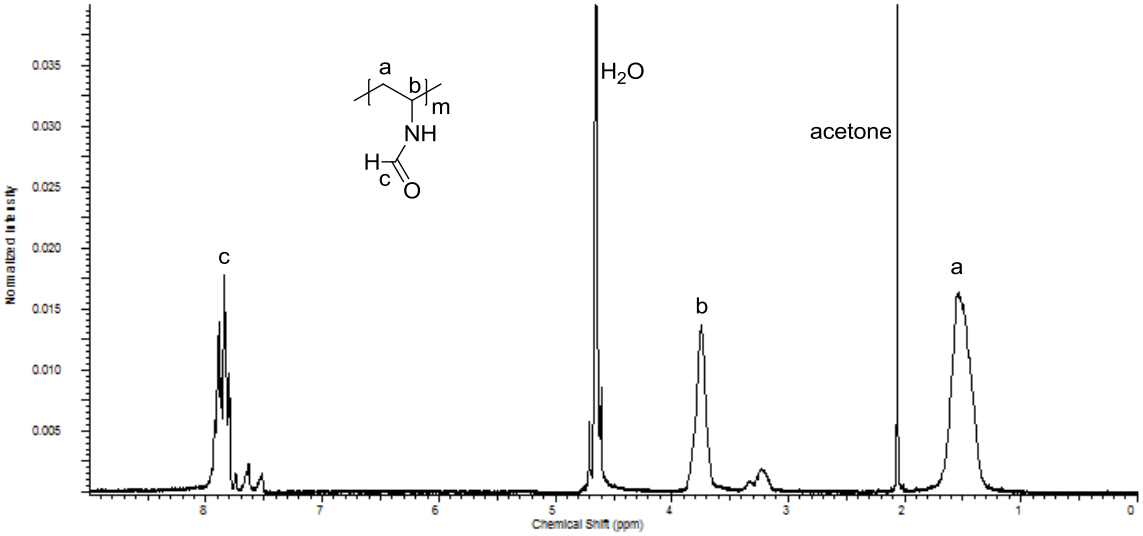

Figure 2.3. 400MHz ^{1}H NMR spectrum of PNVF in D_2O.

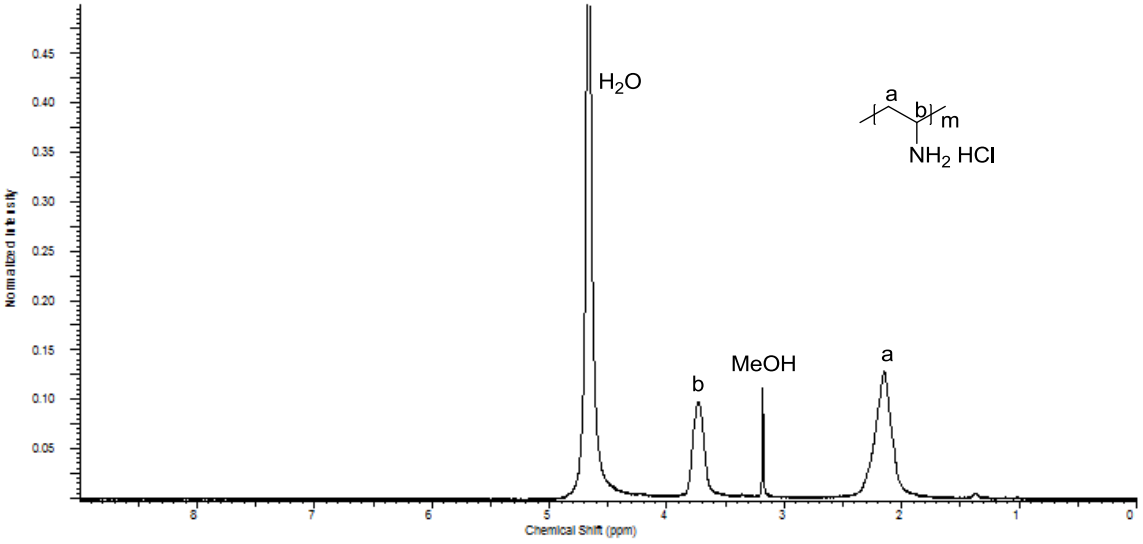

Figure 2.4. 400MHz ^{1}H NMR spectrum of PVAm-HCl in D_2O.

The molecular weight distribution of PNVF was obtained by gel permeation chromatography (GPC). The GPC system was calibrated with poly(acrylamide) (PAM)

standards, since this polymer has a similar structure to PVAm. The number average molecular weight (M_n) and weight average molecular weight (M_w) calibration curves were determined from PAM at various standard molecular masses, as presented in Figure 2.5-2.7 and summarized in Table 2.1. M_n was calculated with equation y = -0.2225x + 53.9. M_w was calculated with equation y = -0.1036x + 53.16, where x is molecular weight (Da) and y is the retention time (min). In this thesis, various molecular weights of PVAm were prepared by altering the initiator type, initiator concentration and solvent (Table 2.2-2.4). It was found that the molecular weight of PNVF decreased with an increase in the monomer: initiator ratio (%) (Table 2.2). The molecular weight distribution of PNVF from GPC is presented in Figure 2.8. As determined by GPC, the PVAm samples appear relatively monodisperse. However, under the conditions used, the PVAm had a high molecular weight in the range of 25,000-109,000 Da, which is unsuitable (too large) for preparation of class 1 CO_2 adsorbent materials.[14]

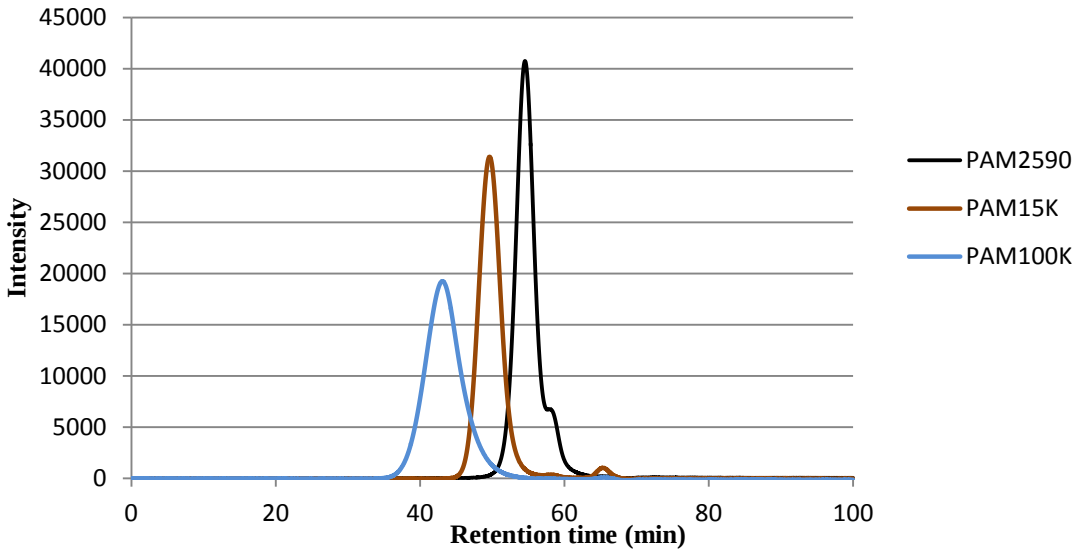

Figure 2.5. Molecular weight distributions of polymer standard poly(acrylamide) (PAM) from GPC.

Table 2.1. Molecular weight distributions of the PAM polymer standard from GPC.

Sample ID	Retention time (min)	M_n	M_w	PDI
PAM2590	54.54	2765	3350	1.21
PAM15K	49.57	12800	15500	1.21
PAM100K	43.15	50000	99000	1.98

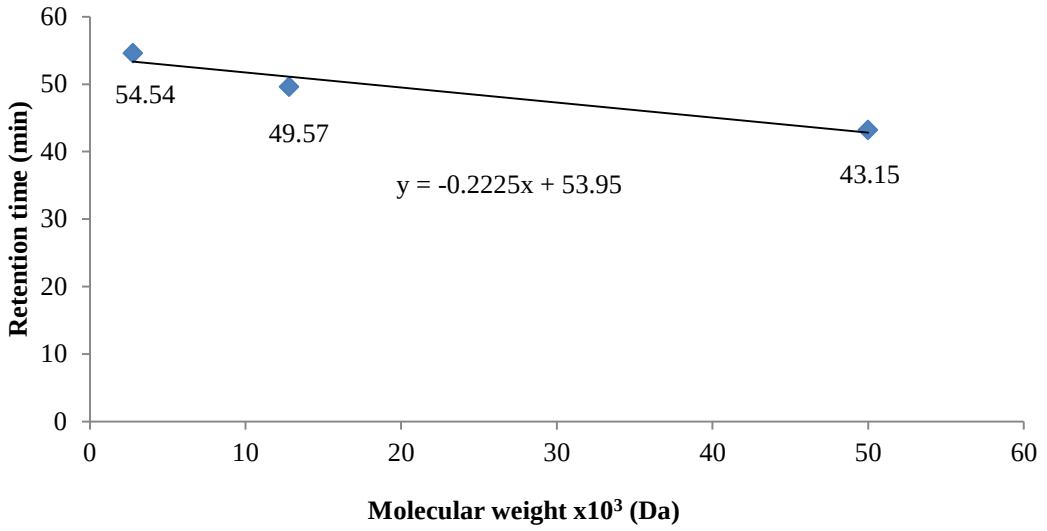

Figure 2.6. The calibration curve of the PAM polymer standard for calculation of M_n.

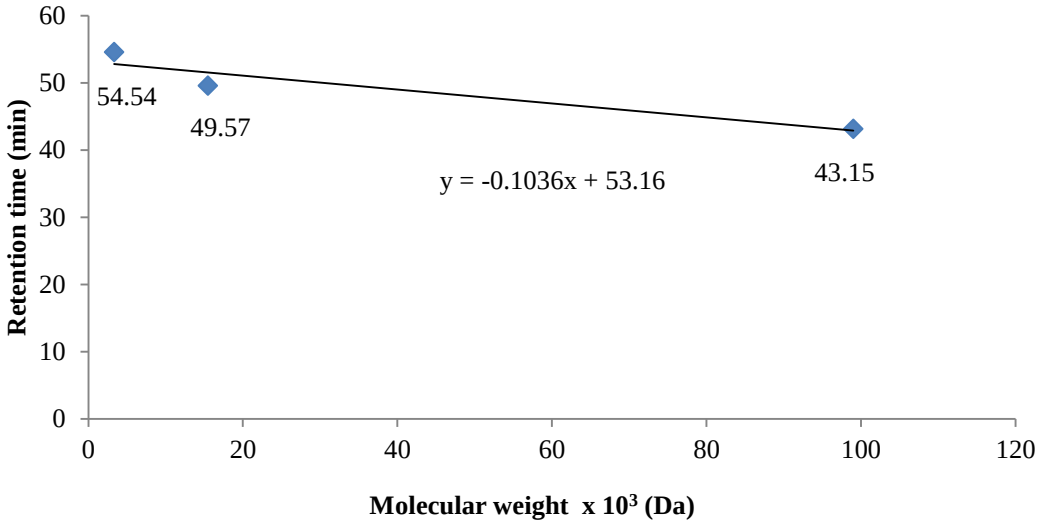

Figure 2.7. The calibration curve of the PAM polymer standard for calculation of M_w.

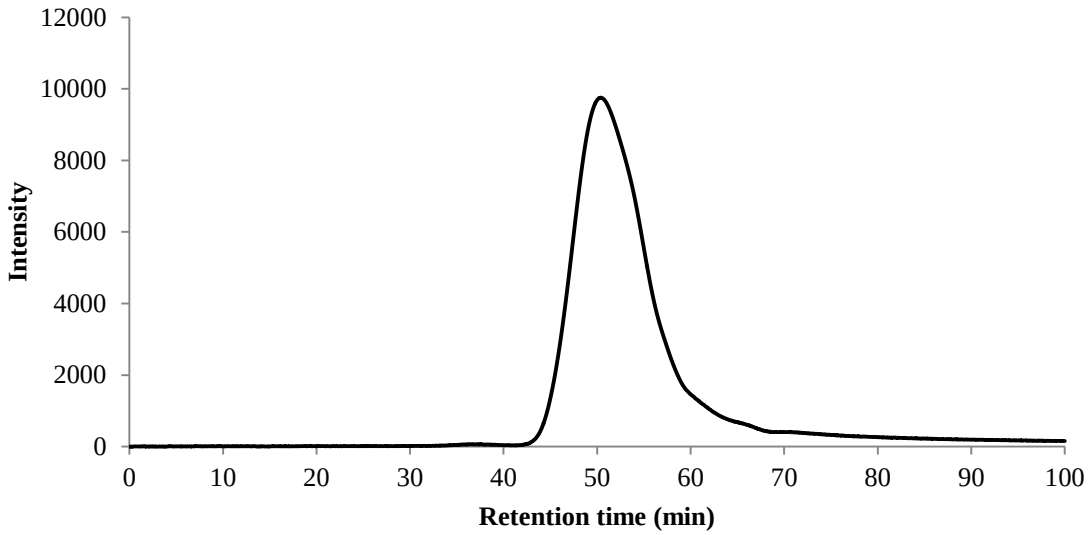

Figure 2.8. Molecular weight distribution of PNVFAIBN-07, retention time 50.57 min.

Table 2.2. Molecular weight distribution of PNVF using AIBN as the initiator.

Sample ID	AIBN (%)	Solvents (ratio)	Retention time (min)	M_w (Da)	M_n (Da)	PDI
PNVFAIBN-01	0.73	H_2O:EtOH(50:50)	41.96	108,108	50,394	2.15
PNVFAIBN-02	1.80	H_2O:IPA, (50:50)	43.30	95,174	47,865	1.99
PNVFAIBN-03	1.80	H_2O:EtOH(50:50)	43.42	94,015	47,326	1.99
PNVFAIBN-04	3.60	H_2O:EtOH(50:50)	44.48	83,784	42,562	1.97
PNVFAIBN-05	4.50	H_2O:EtOH(50:50)	46.94	60,038	31,506	1.91
PNVFAIBN-06	25.00	IPA	48.70	43,050	23,596	1.82
PNVFAIBN-07	30.00	IPA	50.57	25,000	15,020	1.67

Table 2.3. Molecular weight distribution of PNVF using ACPA as the initiator.

Sample ID	ACPA (%)	Solvents (ratio)	Retention time (min)	M_w (Da)	M_n (Da)	PDI
PNVFACPA-01	1.80	H_2O:IPA, 50:50	44.26	85,907	43,550	1.97
PNVFACPA-02	3.00	IPA	46.46	64,672	42,652	1.52

Table 2.4. Molecular weight distribution of PNVF using APH as the initiator.

Sample ID	AAPH (%)	Solvent	Retention time (min)	M_w (Da)	M_n (Da)	PDI
PNVFAAPH-01	1.70	H_2O	41.33	114,093	56,719	2.01
PNVFAAPH-02	1.80	H_2O	41.34	114,093	56,674	2.01

2.3.1.2 Poly(allylamine), PAA

The synthesis of the PAA-HCl was carried out via a one step free- radical polymerization and PAA was obtained after HCl removal using a basic ion-exchange resin. The synthesis route is presented in Figure 2.9.[15]

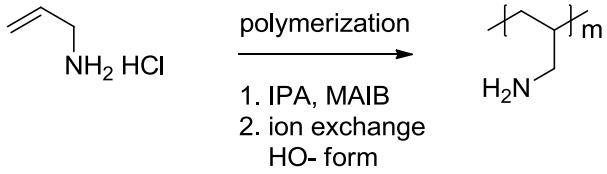

Figure 2.9. Schematic description of the synthesis route of PAA.

Figure 2.10 shows the 400MHz ^{1}H NMR spectrum of PAA-HCl in D_2O. The ^{1}H NMR (400MHz, D_2O, ppm) peaks assignments are as follows: 1.37 (-CH_2-), 1.90 (-CH-), 2.91 (-CH_2-).

The peak integrations in the 400MHz ^{1}H NMR spectra of PAA in a 2:1:2 ratio of (CH_2):(CH):(CH_2) agree with the predicted molecular structure. The NH_2 peak was not observed for PAA-HCl in D_2O because of rapid proton exchange between –NH_2 and any H_2O in D_2O.[16]

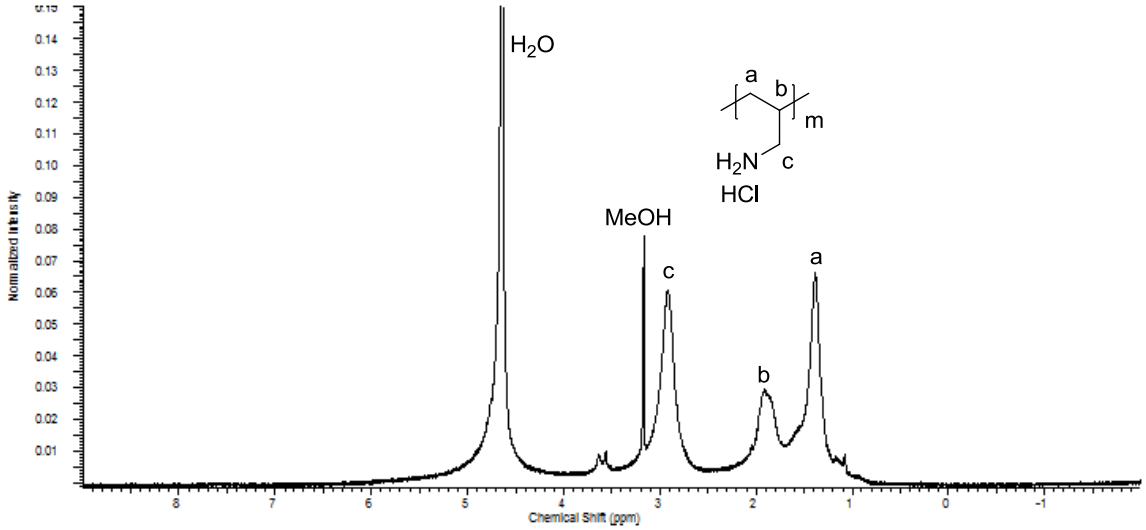

Figure 2.10. 400MHz ^{1}H NMR spectrum of PAA-HCl in D_2O.

Figure 2.11 shows the ^{1}H NMR spectrum of PAA in D_2O. The ^{1}H NMR (400MHz, D_2O, ppm) peak assignments are follows: 1.14 (-CH_2-), 1.52 (-CH-), 2.59 (-CH_2-). As can be seen, the proton resonance peak at 2.85 ppm assigned for the (-CH_2-) of PAA-HCl was shifted to 2.55 ppm in PAA (pH 12), indicating HCl was successfully removed.

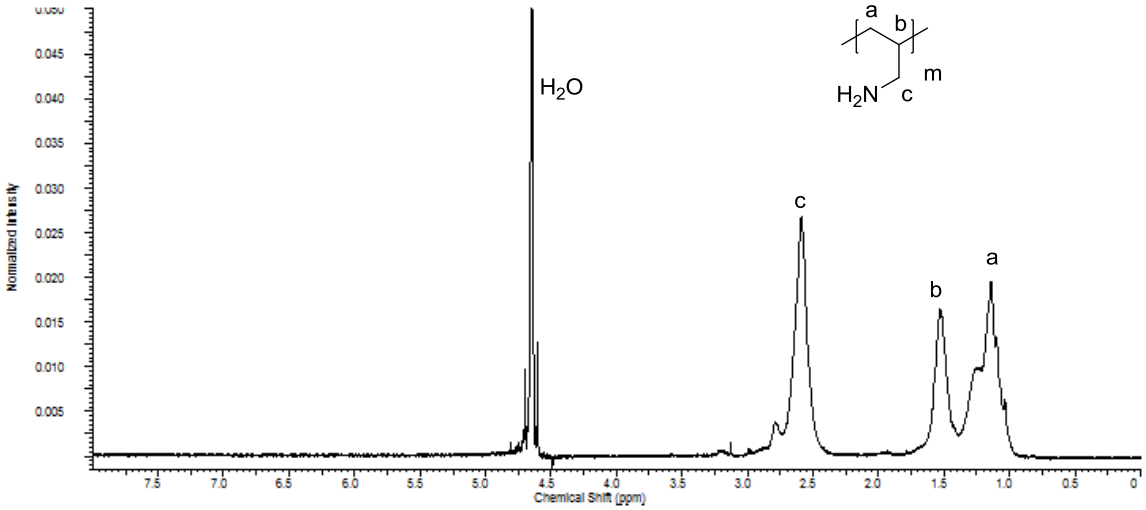

Figure 2.11. 400MHz ^{1}H NMR spectrum of PAA in D_2O.

The molecular weight distribution of PAA was measured by GPC using PAM as the polymer standard, as was done for PVAm. The lowest standard used had a M_n and

M_w of 2765 and 3350 Da, respectively. The PAA samples prepared in this work had lower molecular weights than the standards, and hence, the molecular weight values assigned by GPC are often extrapolated outside the calibration range. Given this fact and that the calibration polymers, PAM, are different from PAA, the molecular weight and PDI data are not rigorously quantitative and should be viewed as only an estimate. Indeed, PDI values of 1, as found below, are not likely accurate and should not be used to infer the polymers produced via uncontrolled radical polymerization are perfectly monodisperse.

The calibration curves used to estimate the M_n and M_w of PAA are presented in Figure 2.12 and 2.13. The figure shows plots of ln e^x versus y, giving the equation $y = (-4.0402x + 59.039)$ to calculate M_n and $y = (-3.5753 + 58.99)$ to calculate M_w, where x is molecular weight (Da) and y is retention time (min). From these calculations, the PAA prepared (retention time 58.55 min) was estimated to have a M_n of 1,130 Da, a M_w of 1,130 Da and a PDI (M_w/M_n) of 1.0. The molecular weight distribution of PAA from GPC is presented in Figure 2.14. As determined by GPC, the PAA sample appears relatively monodisperse. The negative peak derived from the effects of GPC eluent and was not counted in the as molecular weight distribution.[17]

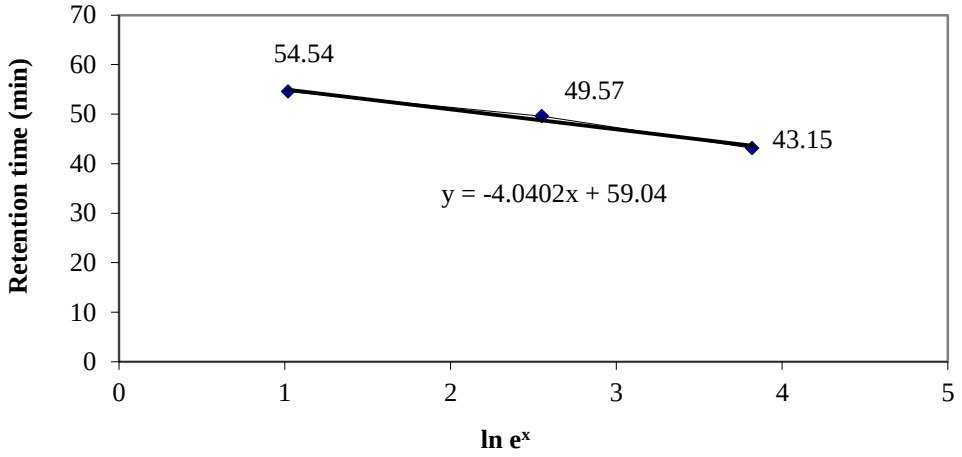

Figure 2.12. The calibration curve of the PAM polymer standard to calculation of M_n.

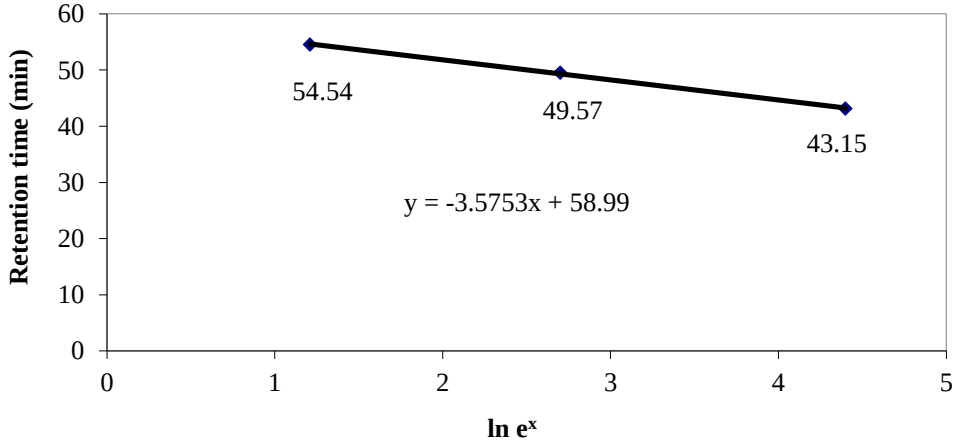

Figure 2.13. The calibration curve of the PAM polymer standard to calculation of M_w.

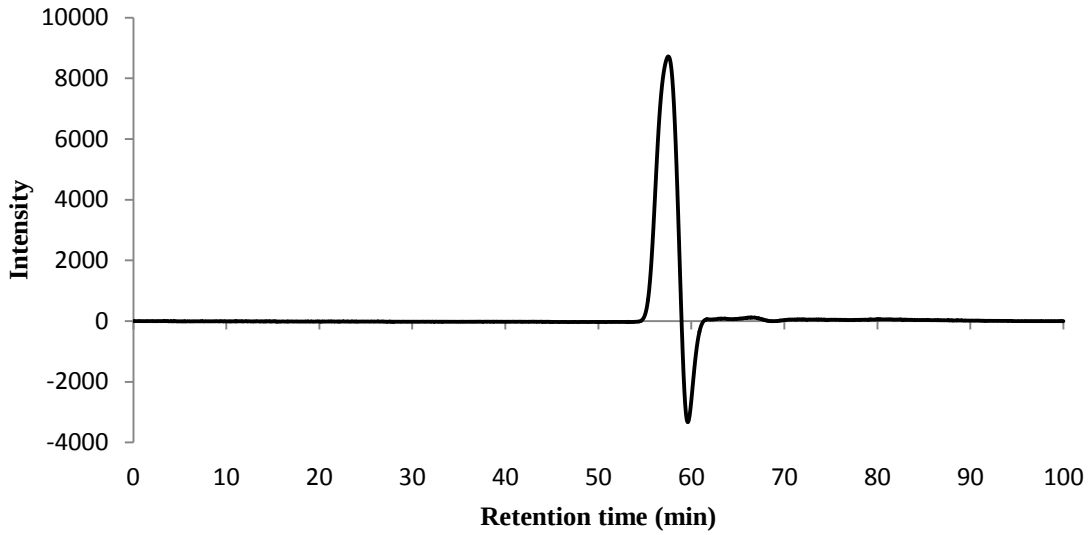

Figure 2.14. Molecular weight distribution of PAA from GPC, retention time 58.55 min.

2.3.2 Characterization of amine-functionalized materials

2.3.2.1 TGA

The thermochemical and physical properties of MCF and the organic loading in the composite adsorbents were assessed by TGA. For the bare MCF material after template removal through calcination, thermogravimetric analysis showed a negligible mass loss of 1.0% attributable to a small amount of silanol condensation. This small mass loss has a negligible effect on subsequent thermogravimetric analyses of the polymer loaded mesoporous materials that are used to assess the organic loadings in the composites. For example, the TGA weight loss curve of bare MCF and various PAA-loaded MCF samples are shown in Figure 2.15. The PAA-loaded MCF samples displayed a mass loss of about 10% over the 27°C-160°C range. This can be attributed to desorption of adsorbed moisture. No obvious mass loss occurred from 160–230°C. The PAA in MCF began to decompose above 230°C in all samples. At about 830°C, the PAA was completely decomposed and fully removed as volatile species. These results

indicate the maximum stability temperature of these samples under these conditions is about 230°C. Other samples were measured in a similar manner.

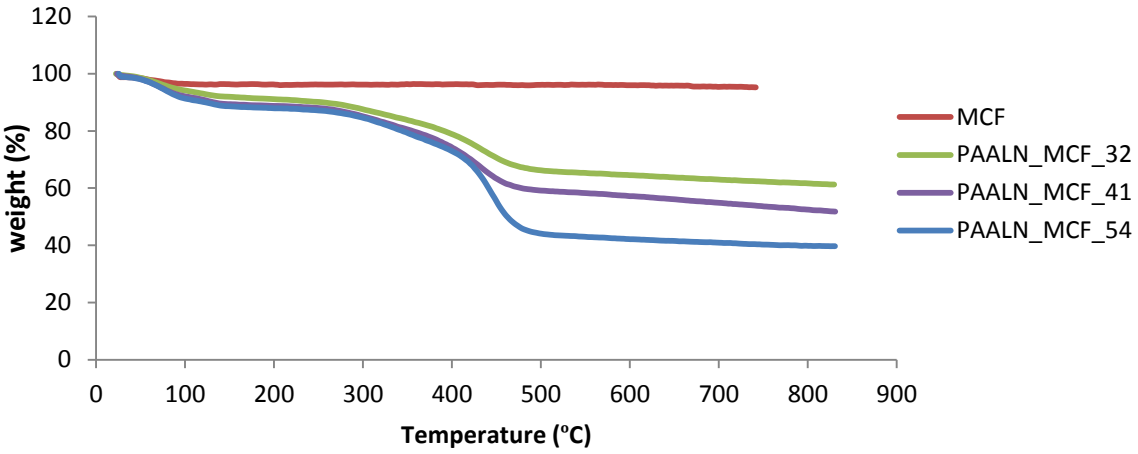

Figure 2.15. TGA profiles of MCF and PAA-loaded MCF samples of different polymer loadings.

2.3.2.2 Nitrogen adsorption/desorption

The surface area, cell diameter, window and pore volume of MCF and the amine polymer-loaded MCF samples were investigated by nitrogen adsorption/desorption isotherms. The textural properties of MCF and the composite samples prepared in this work are presented in Fig 2.17-2.18AZx and are summarized in Table 2.5. As can be seen, all samples exhibit type IV isotherms according to the IUPAC classification. The isotherms demonstrate a significant reduction in total pore volume and surface area with composites containing different polymer percentages. The BET surface area, cell diameter, and window and pore volumes of the bare MCF are 660 m^2/g, 39 nm, 17 nm and 2.7 cm^3/g, respectively. The surface area and pore volume of the composites decrease significantly with increasing polymer loadings.[3] The polymer may be largely contained within the pores, although some part of it could be also outside the pores on the external surface.[18] Together with the TGA results, the data confirm that the amine

polymers are loaded into the pore channels of MCF support to a large extent, but not to the same extent for every polymer at a similar loading.

Table 2.5. Textural properties of MCF materials before and after polymer loading.

Sample ID	**Adsorption Pore volume ($cm^3 g^{-1}$)**	**Desorption Pore volume($cm^3 g^{-1}$)**	**BET surface area (cm^2g^{-1})**
MCF	2.7	2.7	660
PEIBR_MCF_24(1)	2.1	2.1	330
PEIBR_MCF_36(1)	1.5	1.5	221
PEIBR_MCF_53(1)	0.8	0.8	118
PEILN_MCF_22	2.1	2.1	365
PEILN_MCF_37	1.5	1.5	226
PAALN_MCF_32	1.5	1.5	258
PAALN_MCF_41	1.2	1.2	190
PAALN_MCF_54	0.8	0.8	129

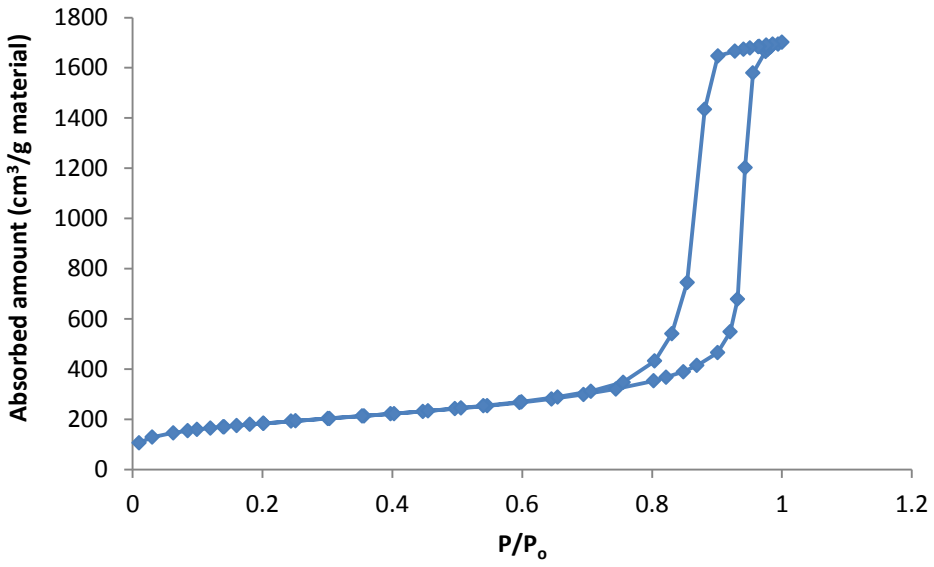

(A)

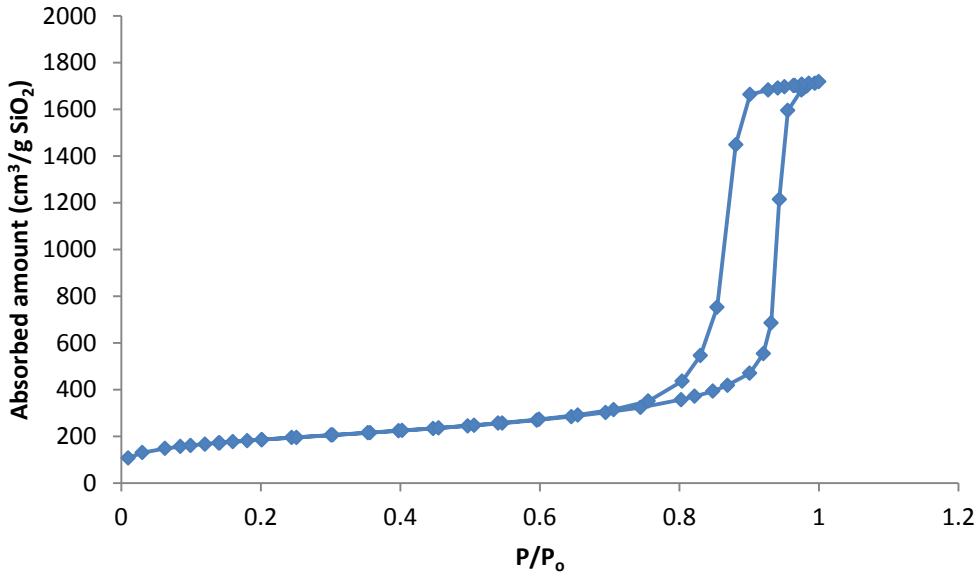

(B)

Figure 2.16. Nitrogen adsorption/desorption isotherm of MCF[II] at 77 K. (A) Absorbed amount plotted based on mass of material, (B) Absorbed amount plotted based on mass of silica.

[II]The MCF isotherm shown here is not from the same batch of MCF used to make the PAALN_MCF adsorbents shown here, but it was made via the same procedure.

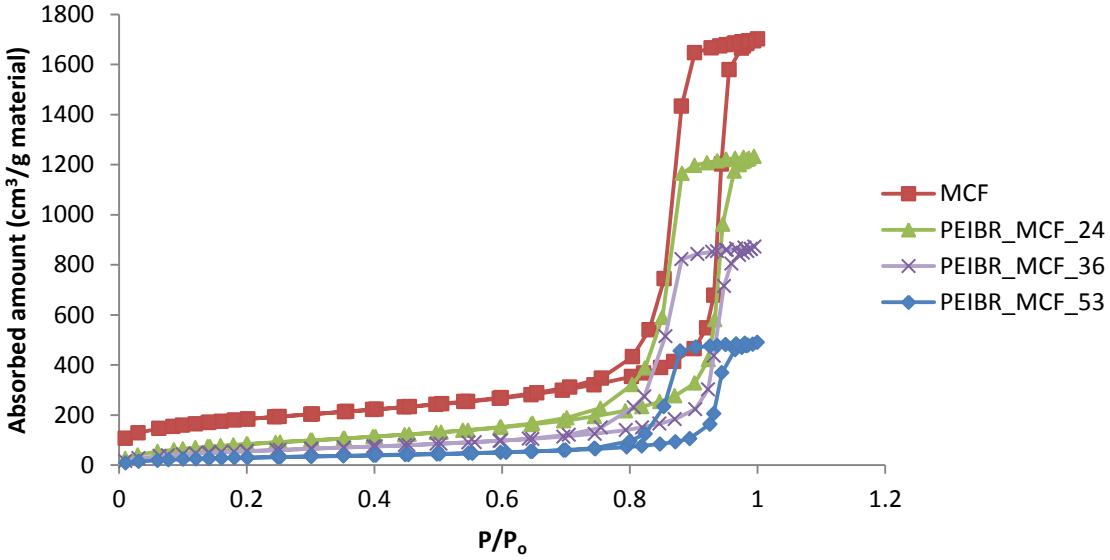

(A)

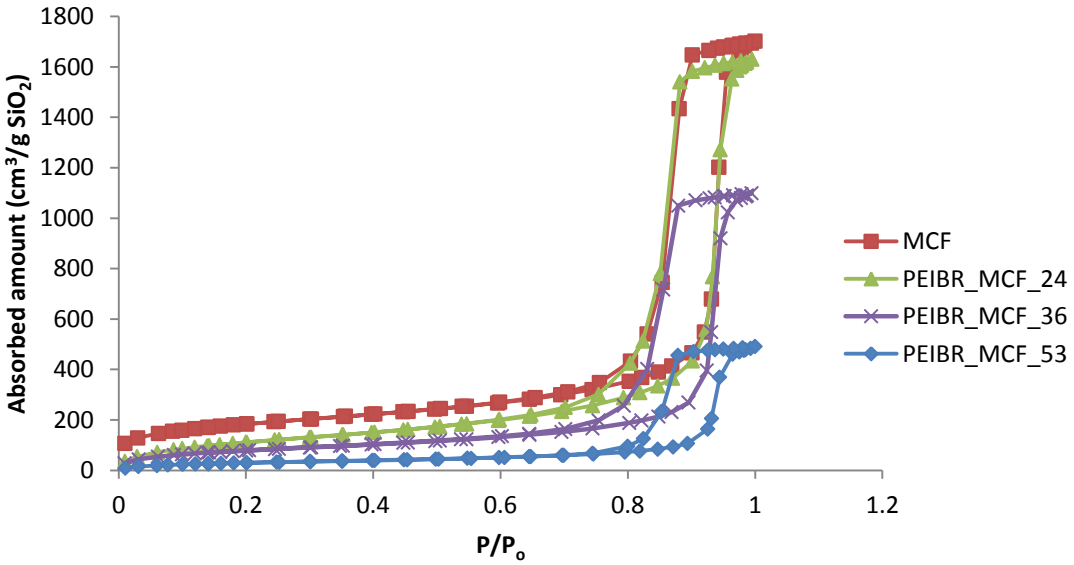

(B)

Figure 2.17. Nitrogen adsorption/desorption isotherms at 77K of samples loaded with branched PEI sample set 1. (A) Absorbed amount plotted based on mass of material, (B) Absorbed amount plotted based on mass of silica.

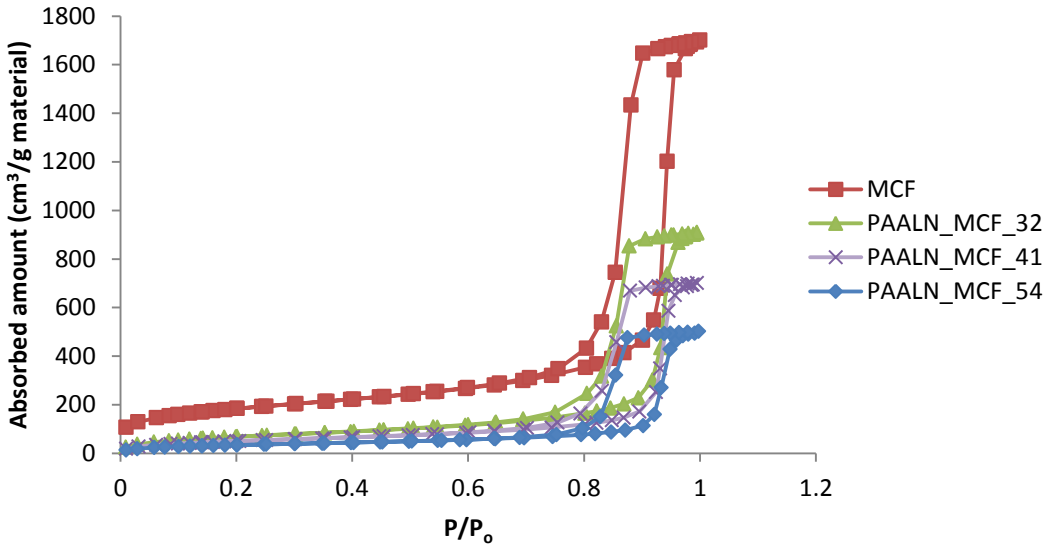

(A)

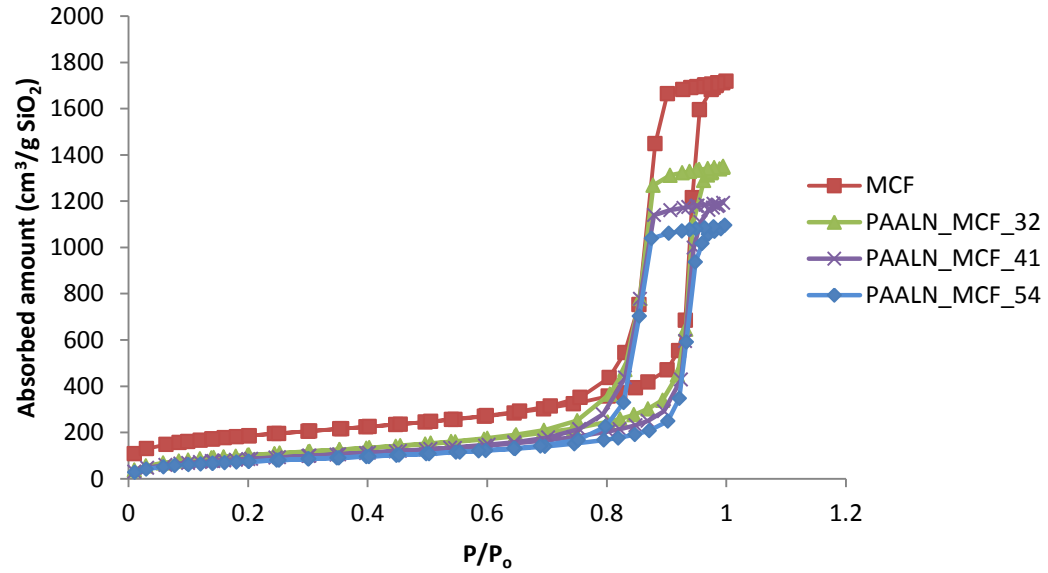

(B)

Figure 2.18. Nitrogen adsorption/desorption isotherms at 77K of samples loaded with linear PAA. (A) Absorbed amount plotted based on mass of material, (B) Absorbed amount plotted based on mass of silica.

2.3.2.3 CO_2 Adsorption

The maximum amine efficiency for CO_2 capture under dry conditions at 10% CO_2 concentration (flue gas conditions) for the branched PEI can be calculated assuming that only primary and secondary amines capture CO_2 under dry conditions, and that two

amines are required to bind one molecule of CO_2. Under such conditions, the maximum theoretical amine efficiency is 0.385 (77% primary and secondary amines). For air capture conditions, using 400 ppm CO_2, it is expected that only primary amines can capture CO_2, making the maximum theoretical amine efficiency 0.22 (44% primary amines). In 10% CO_2, the maximum theoretical amine efficiency for linear PEI is 0.50 (100% primary and secondary amine) and at 400 ppm is 0.02 (3.45% primary amines based on an average of 58 repeat units of M_w 2500 Da.). For linear PAA, which contains all primary amines, the maximum theoretical amine efficiencies are 0.50 for both CO_2 concentrations.

Figure 2.19 presents a comparison of the CO_2 capture performance using 10% CO_2 over branched PEI (sample set 1 and 2), linear PEI and linear PAA loaded MCF materials with different polymer loadings. For branched PEI sample set 1, the adsorption capacity at 28, 38 and 46 wt% loading were 1.21, 1.83 and 2.40 mmol CO_2/g sorbent, respectively. For branched PEI sample set 2, the adsorption capacity at 24, 36 and 53 wt% loading were 1.10, 1.86 and 2.39 mmol CO_2/g sorbent, respectively. At 22 and 37wt% loading, the CO_2 sorption capacities of linear PEI were 0.57 and 1.69 mmol CO_2/ g sorbent, respectively. The CO_2 adsorption capacity increased for all the samples in branched PEI sample set 1, branched PEI sample set 2, and linear PEI samples as the PEI loading was increased. Samples with higher PEI content allowed for larger CO_2 capacities with a roughly linear relationship between capacity and polymer loading, suggesting that the amines are all accessible in these composite samples. The porosity data presented in Table 2.5 and Figures 2.17 are consistent with this supposition. It is noteworthy that branched PEI yielded a higher adsorption capacity than the linear PEI.

For linear PAA, a CO_2 sorption capacity of 1.35 and 1.56 mmol CO_2/g sorbent were measured for 32 and 41wt% loading samples, respectively. The CO_2 sorption capacity decreased as the PAA loading was increased to 54wt% (1.36 mmol CO_2/g sorbent). This could be explained by the difficulty in getting high loadings of linear PAA into the pores, leading to more polymer on the outersurface in a thick film, being less accessible to the CO_2 gas. Low molecular weight branched PEI is a more compact molecule and generally more spherical shapes lead to easier access to the porous structure of the support. In addition, branched PEI contains a large number of reactive terminal primary amine groups, perhaps leading to a lower degree of entanglement resulting amine sites can more fully interact with CO_2 molecules. Unlike low molecular branched PEI, linear PAA has a higher molecular weight, and longer polymer chains. As typical with a linear polymer, the chains adopt a random walk conformation and overlap and entangle with each other.[19-21] Overlapping between polymer chains results entangled polymers that are difficult to access the porosity of the support. Thus, some of them end up deposited out side the pores of the MCF support on the external surface.[22] Moreover, the linear chains can also become entangled inside the pores of support, leading to some amine sites that cannot interact with CO_2 due to steric hindrance, especially at higher loadings, as demonstrated in Figure 2.20.

Table 2.6. Capacity and amine efficiency in 10% CO_2 of the synthesized adsorbent samples.

Sample ID	Amine loading (mmol N/g)	Capacity (mmol CO_2/g sorbent)	Amine efficiency (mmol CO_2/mmol N)
PEIBR_MCF_24(1)	5.67	1.10	0.19
PEIBR_MCF_36(1)	8.44	1.86	0.22
PEIBR_MCF_54(1)	12.45	2.39	0.19
PEIBR_MCF_28(2)	6.49	1.21	0.19
PEIBR_MCF_38(2)	8.96	1.83	0.20
PEIBR_MCF_46(2)	10.71	2.40	0.22
PEILN_MCF_22	5.27	0.57	0.11
PEILN_MCF_37	8.62	1.69	0.20
PAALN_MCF_32	5.74	1.35	0.24
PAALN_MCF_41	7.24	1.56	0.22
PAALN_MCF_54	9.51	1.36	0.14

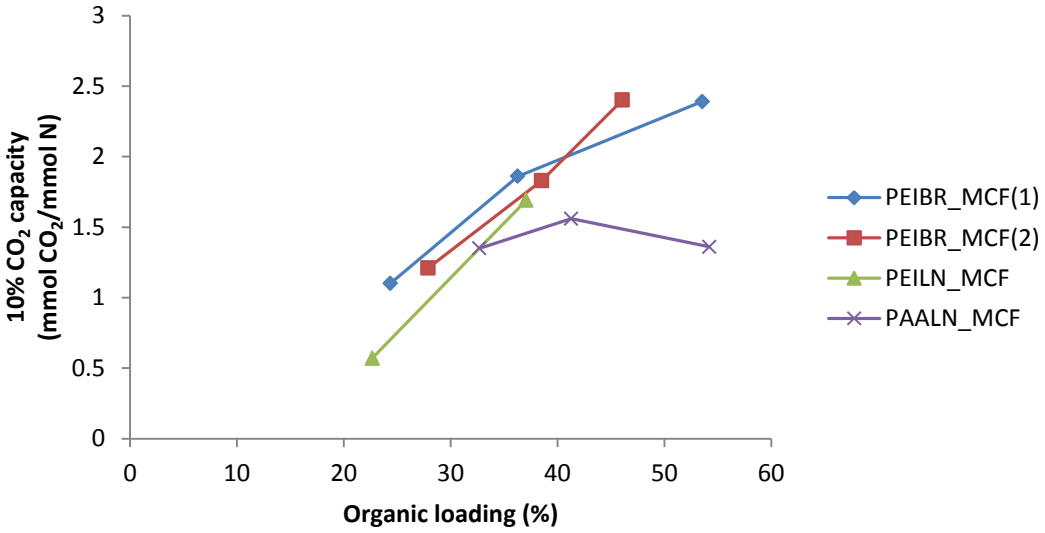

Figure 2.19. CO_2 sorption performance of branched PEI, linear PEI and linear PAA loaded at different organic loadings in 10% CO_2.

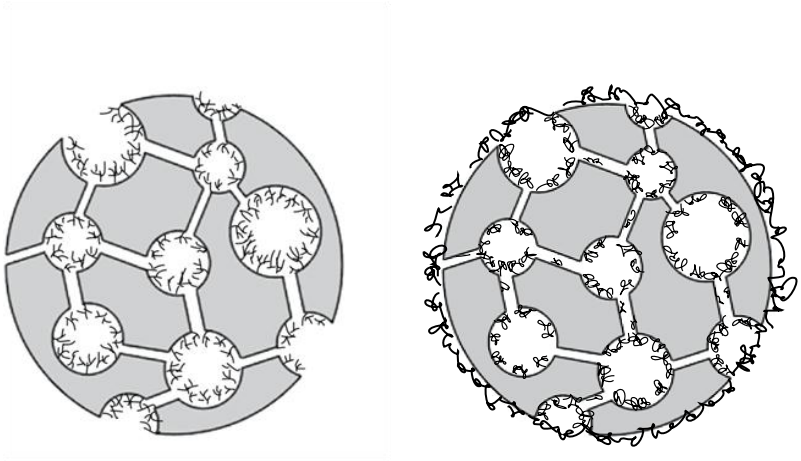

(A) (B)

Figure 2.20. Schematic diagram of polymer loaded in the MCF at high loading . (A) branched PEI (B) linear PAA at high loading.

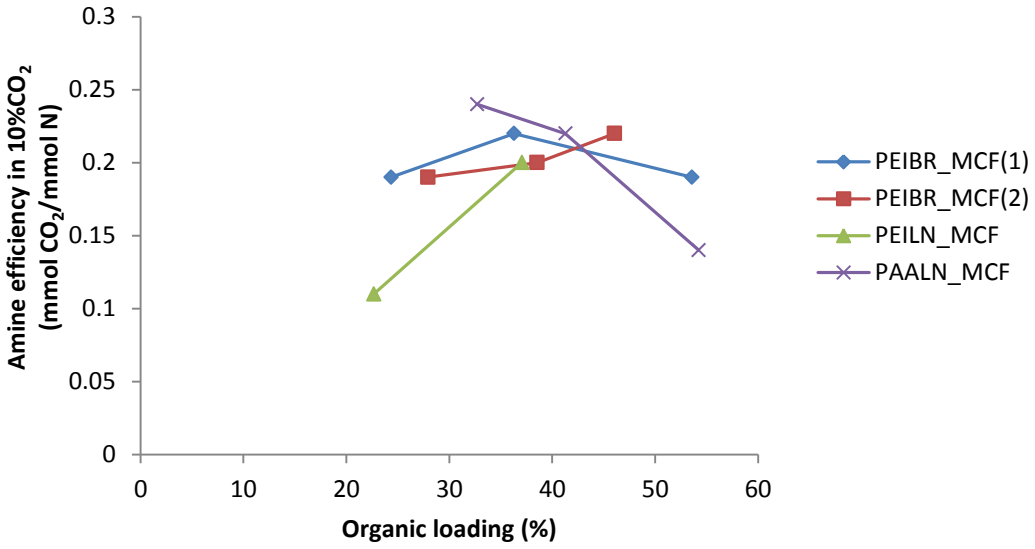

Figure 2.21. Amine efficiency of branched PEI, linear PEI and linear PAA loaded MCF at different organic loadings in 10% CO_2.

Figure 2.21 and Table 2.6 present the amine efficiency of branched PEI, linear PEI and linear PAA composites using 10% CO_2, which show the utilization and accessibility of the amine sites in each composite material. The amine efficiency of the linear PAA sorbents decreased as the organic loading increased. This likely results from the problematic entanglement of the linear chains as suggested above.

Figure 2.22, Figure 2.23 and Table 2.7 present a comparison of the CO_2 capture performance and amine efficiency using a 400 ppm CO_2 gas stream as a function the polymer type (branched PEI, linear PEI and linear PAA) and loading in the MCF support. The adsorption capacity and efficiency of branched PEI increased with increasing loading. Decreasing adsorption capacity and efficiency with increasing polymer loading was observed with linear PAA. Again, as discussed above, the decreased efficiencies are likely associated with amine accessibility which is impacted by polymer branching and molecular weight.

Table 2.7. Capacity and amine efficiency in 400 ppm CO_2 of the synthesized adsorbent samples.

Sample ID	**Amine loading (mmol N/g)**	**Capacity (mmol CO_2/g sorbent)**	**Amine efficiency (mmol CO_2/mmol N)**
PEIBR_MCF_28(2)	6.49	0.61	0.09
PEIBR_MCF_38(2)	8.96	1.08	0.12
PEIBR_MCF_46(2)	10.71	1.74	0.16
PEILN_MCF_22	5.27	0.14	0.03
PEILN_MCF_37	8.62	0.57	0.07
PAALN_MCF_32	5.74	0.63	0.11
PAALN_MCF_41	7.24	0.86	0.12
PAALN_MCF_54	9.51	0.84	0.09

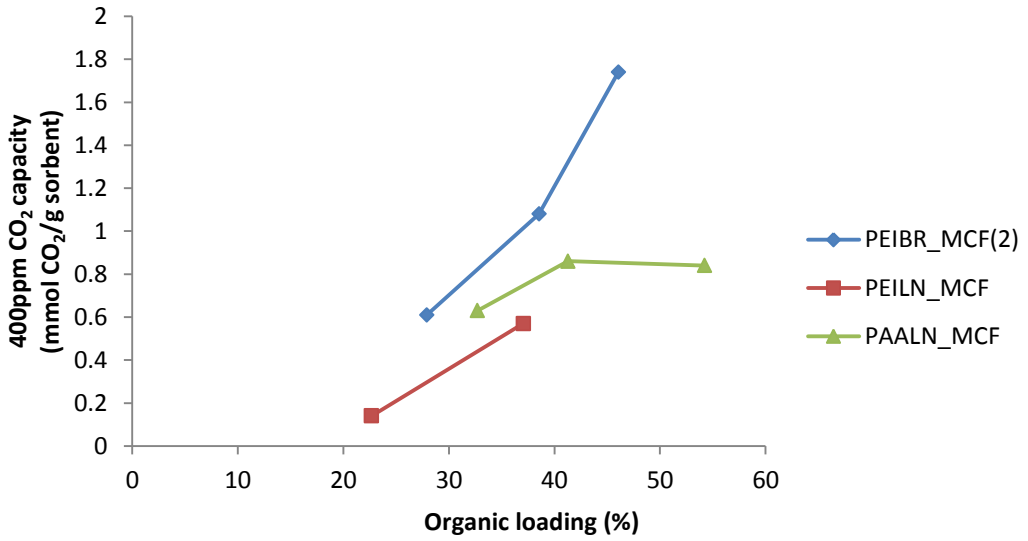

Figure 2.22. CO_2 sorption performance of branched PEI, linear PEI and linear PAA at different organic loadings at 400 ppm conditions.

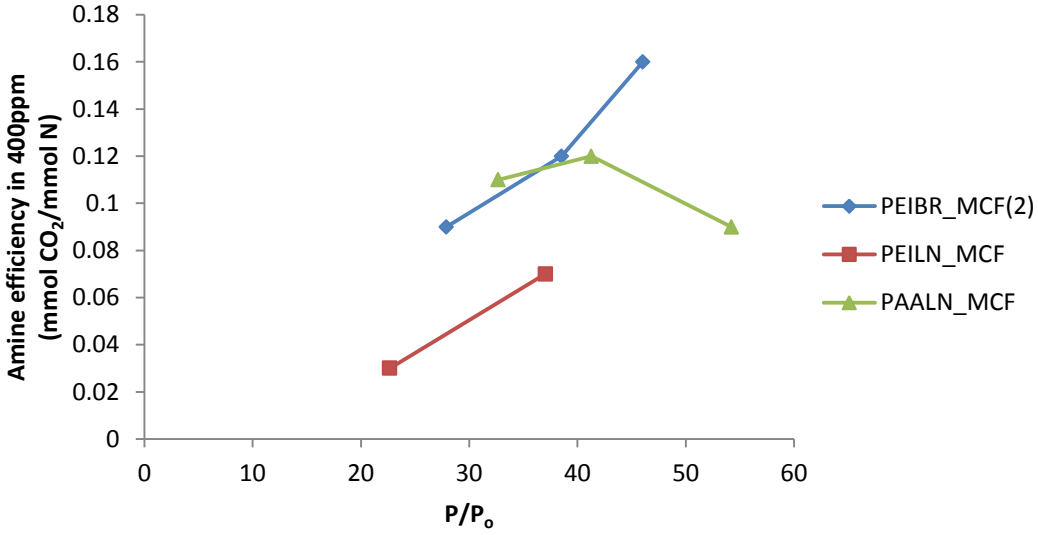

Figure 2.23. Amine efficiency of branched PEI, linear PEI and linear PAA at different organic loadings at 400 ppm conditions.

It should be noted that the order of the utility of the adsorbents is different in comparing results using different partial pressures, 10% CO_2 vs. 400 ppm CO_2. At flue gas conditions, the branched PEI was the most efficient and had the highest capacity, followed by linear PEI and linear PAA. In contrast, the order was branched PEI, then

linear PAA, followed by linear PEI for 400 ppm conditions. This is because linear PEI only has primary amines at the two chain ends and thus there are fewer primary amines in these samples compared to the other two polymers tested. At the lowest polymer loading, the linear PAA is actually more efficient than the branched PEI under 400 ppm conditions, consistent with the hypothesis that primary amines are needed for efficient capture of CO_2 from ultra-dilute gas streams.

2.4 Conclusions

Polymers rich in primary amines, specifically poly(vinylamine) and poly (allylamine), were synthesized and characterized. Subsequently, class 1 materials were prepared for CO_2 capture by impregnating porous silica foams with PAA and various PEIs. The CO_2 adsorption performances were investigated under moderately dilute and ultra-dilute gas streams compared with branched PEI and linear PEI. The results indicate that PAA is a promising to bind CO_2 efficiently, especially ultra-dilute gas stream such as ambient air. However, the linear nature of the polymer precludes its effective use at high polymer loadings, as the polymer cannot be effectively loaded into the silica pores.

2.5 References

1. Choi, S.; Drese, J.H.; Eisenberger, P.M.; Jones, C.W. Application of Amine-Tethered Solid Sorbents for Direct CO_2 Capture from the Ambient Air. *Environ. Sci. Technol*. **2011**, 45, 2420.

2. Li, W.; Choi, S.; Drese, J. H.; Hornbostel, M.; Krishnan, G.; Eisenberger, P. M.; Jones, C. W. Steam-stripping for regeneration of supported amine-based CO_2 adsorbents. *ChemSusChem* **2010**, 3 (8), 899.

3. Xu, X.; Song, C.; Miller, B.G, Scaroni, A.W. Adsorption separation of carbon dioxide from flue gas of natural gas-fired boiler by a novel nanoporous "molecular basket" adsorbent. *Fuel Processing Technology* **2005**, 86, 1457.

4. Ma, X.; Wang, X.; Song, C. Molecular Basket" Sorbents for Separation of CO_2 and H_2S from Various Gas Streams. *J. Am. Chem. Soc.*, **2009**, 131 (16), 5777.

5. Choi, S.; Drese, J. H.; Jones, C. W. Adsorbent materials for carbon dioxide capture from large anthropogenic point sources. *ChemSusChem* **2009**, 2, 796.

6. Rege, S. U.; Yang, R. T.; Buzanowski, M. A. Sorbents for air prepurification in air separation. *Chem. Eng. Sci*. **2000**, 55 (21), 4827.

7. Filburn, T.; Helble, J.J.; Weiss, R.A. Development of Supported Ethanolamines and Modified Ethanolamines for CO_2 Capture. *Ind. Eng. Chem. Res.* **2005**, *44*, 1542.

8. Satyapal, S.; Filburn, T.; Trela, J.; Strange, J. Performance and Properties of a Solid Amine Sorbent for Carbon Dioxide Removal in Space Life Support Applications. *Energy& Fuels* **2001**, 15, 250.

9. Kohn, A.; Nielsen, R.; *Gas Purification*, 5th ed.; Gulf Publishing Co.: Houston, TX, 1997.

10. Lukens,W.; Schmidt-Winkel,P.; Zhao, DY.; Feng,JL.; Stucky,GD. Evaluating Pore Sizes in Mesoporous Materials: A Simplified Standard Adsorption Method and a Simplified Broekhoff−de Boer Method. *Langmuir* **1999**, 15, 5403.

11. Gu, L.; Zhu, S.; Hrymak, A.N. Acidic and Basic Hydrolysis of Poly(N-vinylformamide). *J. Appl. Polym. Sci.* **2002**, 86, 3412.

12. Qui, Y.; Zhang, T.; Ruegsegger, M.; Marchant, R. Novel Nonionoc Oligosaccharide Surfactant Polymres Derived from Poly(vinylamine) with Perdant Dextran and Hexanoyl Groups. *Macromolecules* **1998**, 31, 165.

13. Bromberg,L.; Hatton ,T.A. Poly (N-vinylguanidine):Charaterization, and catalytic and bactericidal properties. *Polymer,* **2007**, 48, 7490.

14. Drage , T.C.; Arenilla, A.; Smith, K.M.; Snape, C.E. Thermal stability of polyethylenimine based carbon dioxide adsorbents and its influence on selection of regeneration strategies. *Micro. Meso. Mater.* **2008**, 116, 504.

15. Kato, T.; Nakata, Y.; Endo, T.; Hayashi, I. Process for the production of allylamine polymer. Patent No. US 6,268,452 B1 2001.

16. Fischer, T.; Heitz, W. Synthesis of polyvinylamine and polymer analogous reactions. *Macromol. Chem. Phys.* **1994**, 195, 679.

17. Thomson Instrument Company. Measurement of Molecular Weight Distribution of Poly (Allylamine) Hydrochloride. http://www.hplc.com/Shodex/english/dc062001.htm.

18. Xu,X.;Novochinskii,I.; Song, C.S. Low-Temperature Removal of H_2S by Nanoporous Composite of Polymer-Mesoporous Molecular Sieve MCM-41 as Adsorbent for Fuel Cell Applications. *Energy Fuels,* **2005**, 19, 2214.

19. Peacock, A.; Calhoun, A. *Polymer Chemistry*. Hanser Gardner Publications, Cincinnati, 2006.

20. Kapnitos, M.; Lang, M.; Vlassopoulos, D.; Pyckhoit-Hinzen, W.; Richter, D.; Cho, D.;Chang, T.;Rubinstein, M. Unexpected power-law stress relaxation of entangled ring polymers. *Nature Materials*, **2008**, 7, 997.

21. Kroger, M.; Voigt, H. On a quantity describing the degree of chain entanglement in linear polymer systems. *Macromol. Theory Simul*. **1994**, 3, 639.

22. Xu, X.; Song, C.; Andresen, J.M.; Miller, B.; Scaroni, A.W. Preparation and characterization of novel CO_2 "molecular basket" adsorbents based on polymer-modified mesoporous molecular sieve MCM-41. *Micro. Meso. Mater*. **2003**, 62, 29.

CHAPTER 3

CROSS-LINKED, BRANCHED AND FUNCTIONALIZED PRIMARY AMINE-RICH POLYMERS FOR CO_2 CAPTURE FROM FLUE GAS OR ULTRA-DILUTE GAS STREAMS SUCH AS AMBIENT AIR

3.1 Introduction

From discussion in Chapter 2, primary amine poly(allylamine) (PAA) is a promising new material for binding CO_2 efficiently, especially from ultra-dilute gas streams such as ambient air. However, the linear nature of the polymer appears to inhibit its effective use at high loadings, compared with branched poly(ethyleneimine) (PEI), as the polymer cannot be as effectively loaded into the silica pores and the linear chains may entangle in such a way inside the pores of the support to hinder the accessibility to CO_2 molecules. On the basis of the results of Chapter 2, a study was initiated to evaluate the transformation of linear PAA to other structures to potentially alter the accessibility of the amine sites ideally leading to improved CO_2 adsorption capacities and amine efficiencies. Cross-linking and branching of polymer chains are well known ways to modify the structure of linear polymers to alter their properties in a variety of applications.[1,2] Thus, the goal of the work described in this chapter is to assess the impact of polymer cross-linking and branching. This study hypothesize that alternating the structure of linear PAA by cross-linking and branching will be a promising way to improve the CO_2 adsorption performance in moderately dilute and ultra-dilute gas streams.

3.2 Experiment

3.2.1 Materials

The following chemicals were used as received from the supplier: Allylamine hydrochloride (AAHCl, TCI), isopropanol anhydrous (IPA, 99.5%, Alfa Aesar), methanol (MeOH, 99.5%, Sigma Aldrich), 2,2-azobisiobutyric acid dimethyl ester (MAIB, 98%, AK Scientific), epichlorohydrin (EPI, 99.5%, Sigma Aldrich), strongly basic ion exchange resin (Ambersep 900 OH^- form, Sigma-Aldrich), poly(acrylamide) GPC standards (PAM2950, PAM15K, PAM100K, American Polymer Standards), water for GPC (TraceSelect, Sigma Aldrich), Pluronic P123 EO-PO-EO triblock copolymer (P123, Sigma-Aldrich), 1,3,5-trimethylbenzene (TMB, 97%,Sigma-Aldrich), tetraethyl orthosilicate (TEOS, 98%,Sigma-Aldrich), ammonium fluoride (NH_4F, >96%, Alfa Aesar), hydrochloric acid (HCl, conc. 37%, J.T. Baker), divinylbenzene (DVB, 80% Alfa Aesar). DVB was washed with 4% NaOH (30 mL, 3 times) and with water (30 mL, 3 times) to remove the inhibitor before use.

3.2.2 Synthesis of Polymers

3.2.2.1 Synthesis of poly(allylamine), PAA

The solution of allylamine hydrochloride (6g, 0.06mol), isopropanol (3.99g) and MAIB (0.79g, 3.43mmol) was deaerated by argon purging for 1h. The polymerization was carried out at a constant temperature of 60°C for 48h. The resulting polymer was washed with excess methanol to remove unreacted monomer. PAA-HCl was recovered by filtration and dried under vacuum at room temperature for 24h to give 4.50g of white powder (70%). ^{1}H NMR (400MHz, D_2O, ppm): 1.37 (-CH_2-), 1.90 (-CH-), 2.91 (-CH_2-).

PAA was obtained by using a strongly basic ion exchange resin OH^- form to remove the HCl. Additional degassed deionized water (30mL) and 16g strongly basic ion exchange resin were added to the mixture and stirred for 1h. The resulting polymer solution at pH 12 was filtered, the solvents were removed by vacuum and the polymer dried under vacuum for 24h to give 4.0g of product (60%). ^{1}H NMR (400MHz, D_2O, ppm): 1.14 -CH_2-), 1.52 (-CH-), 2.59 (-CH_2-).

3.2.2.2 Synthesis of cross-linked poly(allylamine) using epichlorohydrin, PAAEPI

A 20% w/v solution of linear PAA-HCl was prepared by mixing under argon atmosphere. PAA-HCl (2.0g, 0.02mol) and degassed deionized water (8.0g) were mixed. NaOH (0.72g) was added. When the temperature of the solution dropped to ambient temperature (the dissolution of NaOH is exothermic), EPI 84uL (1.07 mmol) was added. The reaction mixture was vigorously stirred for 16 h and slowly stirred for an additional 2h. The cross-linked PAAEPI was obtained by using the strongly basic ion exchange resin OH^- form to remove the HCl. Additional degassed deionized water (30mL) and strongly basic ion exchange resin (16g) were added to the mixture and stirred for 1h. The resulting solution of cross-linked PAA polymer at pH 12 was filtered, the solvent was removed by vacuum and the polymer was dried under vacuum for 24h to give 1.8g product (90%). ^{1}H NMR (400MHz, D_2O, ppm): 1.19 (-CH_2-), 1.62 (-CH-), 2.65 (-CH_2-), 3.85 (-CHO).

3.2.2.3 Synthesis of branched poly(allylamine) using divinylbenzene, PAADVB

The solution of allylamine hydrochloride (1.5g, 0.016mol), isopropanol (1g), MAIB (0.2g) and divinylbenzene (0.0106g) was deaerated by argon purging for

1h. The polymerization was carried out at a constant temperature of 60°C for 48h. The resulting polymer was washed with excess methanol to remove unreacted monomer. PAADVB-HCl was recovered by filtration and dried under vacuum at room temperature for 24h to give 1.2g of white powder (80%).

PAADVB was obtained by using a strongly basic ion exchange resin OH^- form to remove the HCl. Additional degassed deionized water (20mL) and strongly basic ion exchange resin (12g) were added to the mixture and stirred for 1h. The resulting polymer solution at pH 12 was filtered, the solvent was removed by vacuum and the polymer dried under vacuum for 24h to give 1.1g of product (91%). ^{1}H NMR (400MHz, D_2O, ppm) 1.25 ($-CH_2-$), 1.76 (-CH-), 2.79 ($-CH_2-$), 7.52 (Ar)

3.2.3 Synthesis of Silica Mesocellular Foam, MCF

A solution of P123 (16.0g), water (260g) and concentrated HCl (47.4g) were stirred for 24h to complete copolymer dissolution. The flask was then transferred to a 40°C oil bath and TMB (1.6g) was added. The mixture was stirred at 40°C for 2h, then TEOS 34.6g were added. The solution was stirred an additional 5 min and then left quiescent for 20h at 40°C. A solution of NH_4F 184mg in deionized water (20mL) was added as a mineralization agent, and the mixture was swirled for 5 min before aging at constant temperature of 100°C for 24h. The resulting precipitate was filtered, washed with excess water, dried, and calcined in air at 550°C for 6h (1.2°C/ min ramp). A typical silica MCF was obtained, 15g (95%).

3.2.4 Impregnation of Polymers in MCF

The amine polymer-loaded MCF samples in different weight percentage loadings were prepared by a wet impregnation method. In a typical preparation, the desired

amount of amine polymer was dissolved in methanol under stirring for about 15 min while purging the mixture with argon gas, until the polymer dissolved completely. Then, the necessary amount of calcined MCF was added to the mixture. The resulting mixture was stirred for 16h under an argon atmosphere. The mass ratio of methanol:MCF was always maintained constant at 28:1 for each sample, while the ratio of MCF: polymer was varied in each case. The resulting final solid was recovered by removal of the solvent under vacuum and drying under vacuum at ambient temperature for 24h. The as-prepared adsorbents were denoted as X_MCF_Y, where X represents the amine polymer, Y represents the polymer weight percentage in the sample. Linear PAA, cross-linked PAAEPI, and branched PAADVB are referred to as PAALN, PAAEPICL, and PAADVBBR, respectively.

3.2.5 Characterization

The polymer structure was characterized using solution ^{1}H NMR. The measurements were performed using a Mercury Vx 400MHz with D_2O as solvent. Molecular weights of the polymers were determined by gel permeation chromatography, GPC, at 30°C. The GPC system was comprised of a Shimadzu LC-20AD pump, a Shimadzu RID-10A RI detector, a Shimadzu SPD-20A UV detector, a Shimadzu CTO-20A column oven, and Viscotek TSK Viscogel PWXL Guard, G3000, G4000, and G6000 columns mounted in series. The mobile phase consisted of 0.05*N* $NaNO_3$ and the flow rate was maintained at 0.4 mL/min. Poly (acrylamide) standards were used (M_w 3350, 15500, 99000), (M_n 2765, 12800, 45600). The surface area, total pore volume and pore size distributions of the oxide support and oxide-supported polymers were determined by nitrogen adsorption–desorption isotherm measurements at 77K using a

Micromeritics TRISTAR2002. The samples were degassed under vacuum at 100°C overnight before the adsorption measurements. The surface area was determined by the Brunauer–Emmett–Teller (BET) method. Total pore volume, and cell and window pore size were calculated using the Broekhoff-de Boer method with the Frenkel–Halsey–Hill (BdB-FHH) modification.[3] Total pore volume was calculated from the amount of absorbed nitrogen at P/P_o=0.99. The organic loading of the materials was characterized by combustion using a Netzsch STA409 TGA under a flowing nitrogen diluted air stream. About 10 mg of the sample was heated from 27-740°C at a rate of 10°C/min.

3.2.6 CO_2 Adsorption

The CO_2 adsorption characteristics of the amine polymer-loaded MCF materials were characterized using a TA Q500 thermogravimetric analyzer. A sample weight of about 20 mg of sorbent was loaded in a platinum vessel and tested for CO_2 adsorption performance. The initial activation of the sample was carried out at 120°C for 3h after heating to that temperature at 5°C/min rate under an Ar flow of a 100 ml/min. Then, the temperature was decreased to 25°C and held for 1h at that temperature before introducing CO_2. Adsorption was then initiated by exposing the samples to the dry target gas of desired concentration (400 ppm CO_2 or 10% CO_2 balanced with Ar) at a flow rate of 100 ml/min. The adsorption experiment was performed until the pseudo-equilibrium capacity was reached, which was determined to be the time when the weight gains from adsorbed CO_2 changed by less than 0.0001 %/min. The adsorption runs were conducted for 12h for 400 ppm gas experiments and 3h for 10% CO_2 experiments.

3.3 Results and Discussion

3.2.1 Characterization of the polymer

3.2.1.1 Cross-linked poly(allylamine) using epichlorohydrin, PAAEPI

The randomly cross-linked poly(allylamine) was prepared by mixing a 20% w/v aqueous solution of linear PAA-HCl and the cross-linking agent epichlorohydrin (EPI). PAA-HCl chains contains hydrochloric acid (HCl) ionically associated with amine (NH_2) groups along the polymer chain backbone. Before crosslinking, the polymer chains containing of the HCl groups were neutralized with NaOH to provide free NH_2 sites for the EPI crosslinking reaction. Under the conditions used in this work, PAAEPI is only lightly cross-linked, remaining water soluble. The crosslinking synthesis routes of PAAEPI are presented in Figure 3.1.

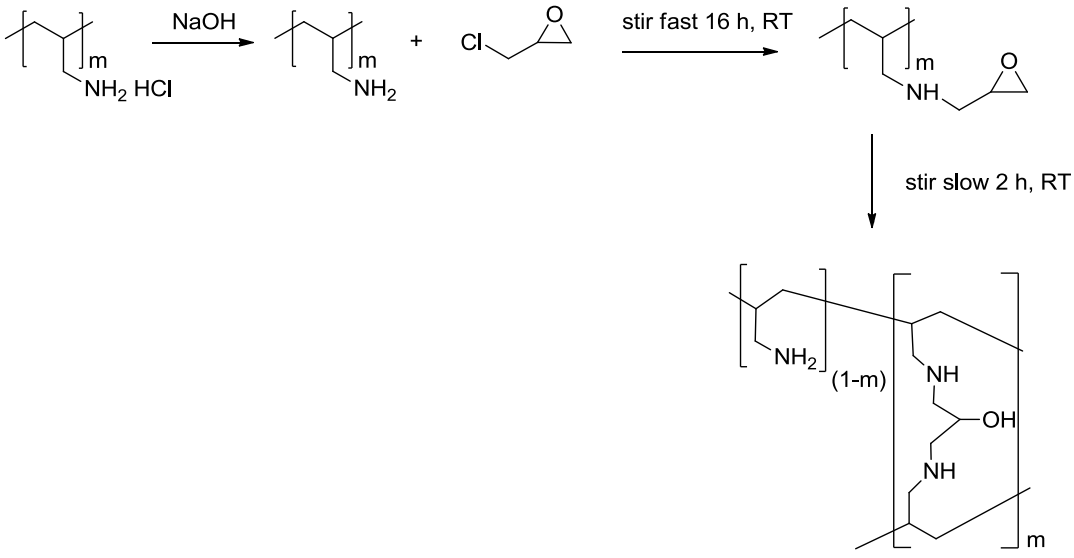

Figure 3.1. Schematic description of the synthesis route of cross-linked PAAEPI.[5]

Figure 3.2 shows the ^1H NMR spectrum of cross-linked PAAEPI in D_2O. The ^1H NMR (400MHz, D_2O, ppm) peak assignments are as follows: 1.19 ($-CH_2-$), 1.62

(-CH-), 2.65 (-CH_2-), 3.85 (-CHO-). As can be seen, the proton resonance peak at 3.85 ppm assigned to proton of epichlorohydrin indicate cross-linked PAAEPI was successfully synthesized.[4] The degree of cross-linking of PAAEPI was calculated from the integral area ratio of the methine peak at 3.85 ppm (-CHO-) to that at 2.65 ppm (-CH_2-). The peak integrations yielded the ratio in a 19:1 of (-CH_2-):(-CHO-) indicating that the polymer chain 19 repeating units of PAA incorporate 1 repeating unit of EPI.

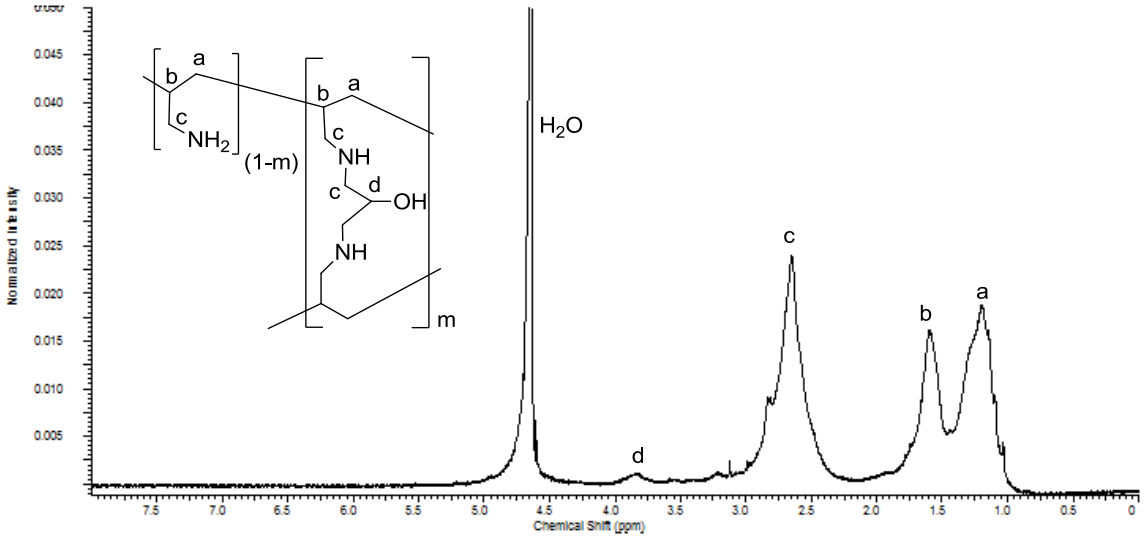

Figure 3.2. 400 MHz ^{1}H NMR spectrum of cross-linked PAAEPI in D_2O.

The molecular weight distribution of cross-linked PAAEPI was measured by GPC using PAM as the polymer standard, as was done for PAA (see Chapter 2). The calculation of M_n and M_w were applied using the same equations as for PAA. From these calculations, the parent PAA-HCl prepared (retention time 58.55 min) was estimated to have a M_n of 1,130 Da, a M_w of 1,130 Da and a PDI (M_w/M_n) of 1.0.[I]

[I] Note that the lowest Mn and Mw standard used here is poly(acrylamide) of ca.2765 and 3350 Da, respectively. Many polymers produced here are of lower molecular weight, hence, molecular weight data are often extrapolated outside the calibration range. Given this fact and that the calibration polymers are of different type [poly(acrylamide)], the molecular weight and PDI data are not rigorously quantitative and should be viewed as a very rough estimate.

The cross-linked PAAEPI prepared (retention time 58.38 min) was estimated to have a M_n of 1,180 Da, a M_w of 1,190 Da and a PDI (M_w/M_n) of 1.0.[I] Figure 3.3 shows the molecular weight distribution of cross-linked PAAEPI from GPC. As determined by GPC, the cross-linked PAAEPI sample appears relatively monodisperse. The shoulder of the peak may be derived from solvent.

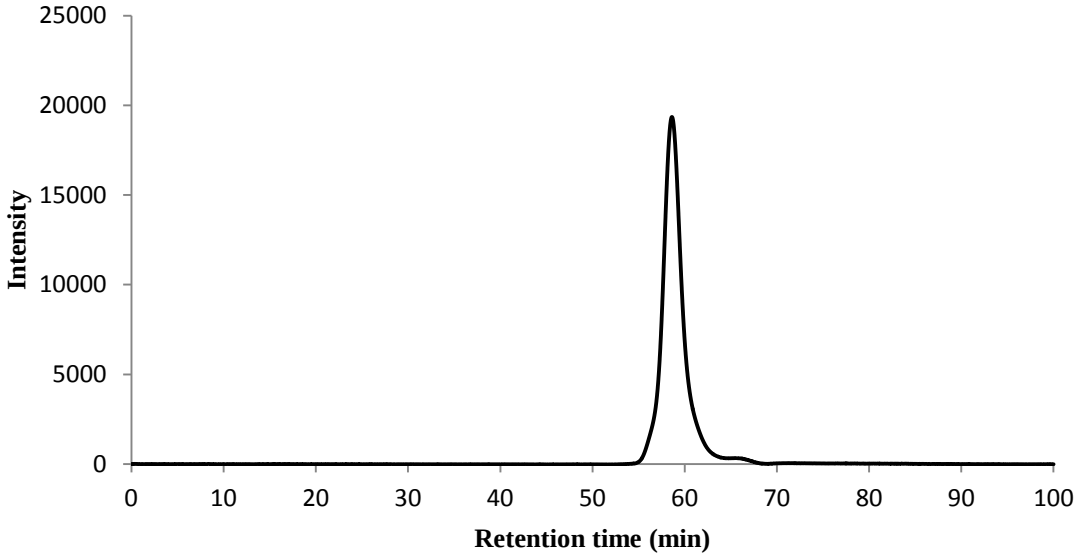

Figure 3.3. Molecular weight distribution of cross-linked PAAEPI, retention time 58.38 min.

3.2.1.2 Branched poly(allylamine) using divinylbenzene, PAADVB

The synthesis of the branched PAADVB was carried out via a one step free-radical polymerization using divinylbenzene (DVB) served as the branching agent. The synthesis route is presented in Figure 3.4. Figure 3.5 shows the ^{1}H NMR spectrum of branched PAADVB in D_2O. The ^{1}H NMR (400MHz, D_2O, ppm) peak assignments are as follows: 1.25 (-CH_2-), 1.76 (-CH-), 2.79 (-CH_2-), 7.52 (Ar). As can be seen, the proton resonance peak at 7.52 ppm assigned for the proton of aromatic ring indicating that branched PAA using divinylbenzene was successfully synthesized. The degree of

branching of PAADVB was calculated from the integral area ratio of the protons signal peak at 7.52 ppm (Ar) to that at 2.79 ppm (-CH_2-). The peak integrations yielded the ratio in a 70:1 of (-CH_2-):(Ar) indicating that the polymer chain 70 repeating units of PAA incorporate 1 repeating unit of DVB.

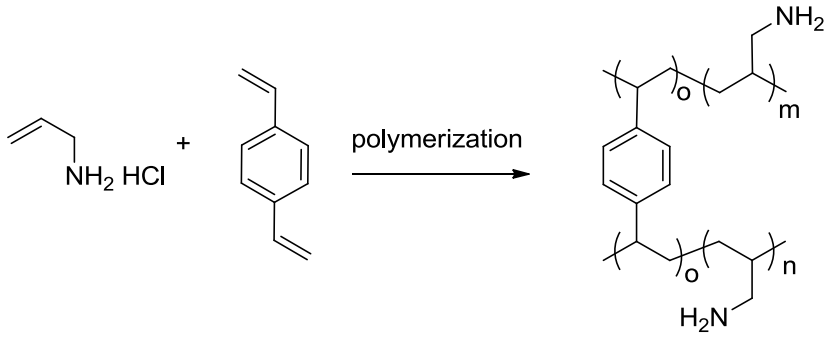

Figure 3.4. Schematic description of the synthesis route of branched PAADVB.

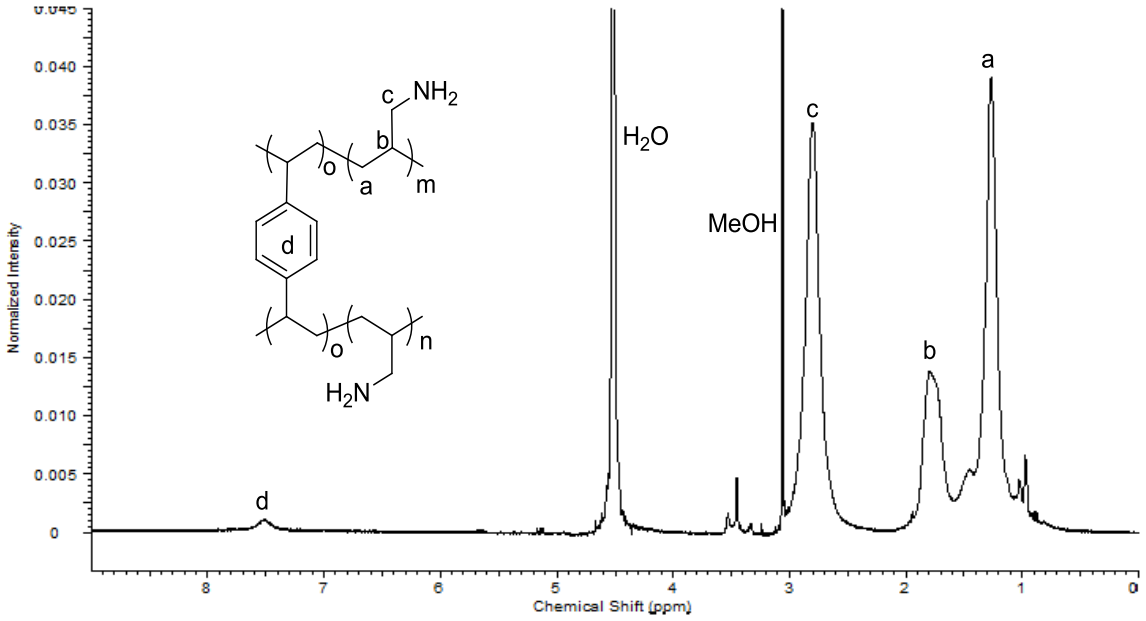

Figure 3.5. 400 MHz ^{1}H NMR spectrum of branched PAADVB in D_2O.

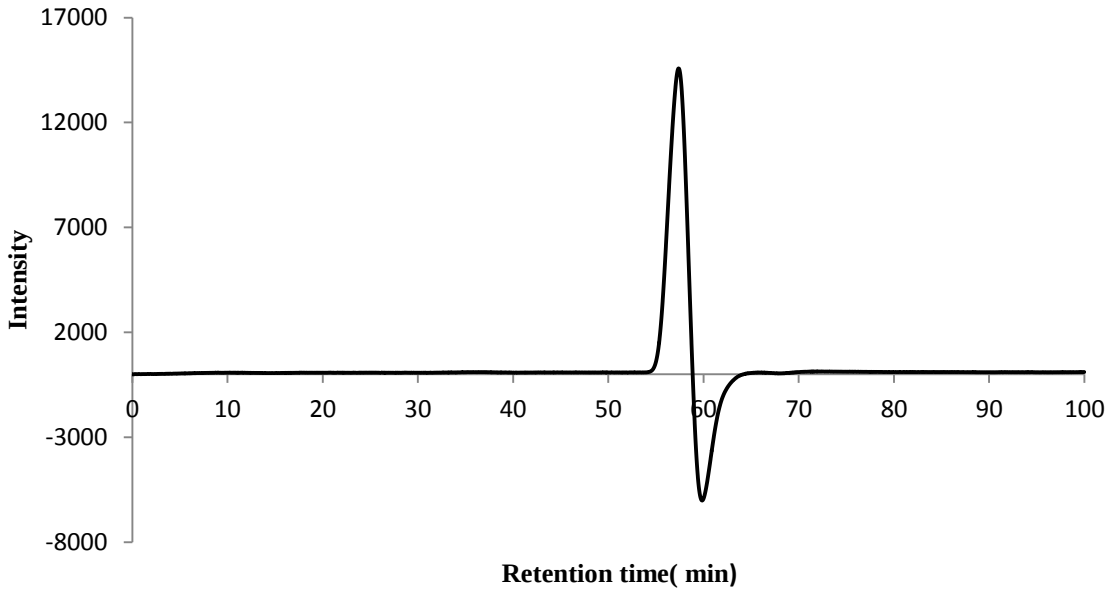

Figure 3.6. Molecular weight distribution of branched PAADVB, retention time 57.45 min.

The molecular weight distribution of branched PAADVB was measured by GPC using PAM as the polymer standard, as was done for PAA (see Chapter 2). The calculation of M_n and M_w were applied using the same equations as for of PAA. From these calculations, the branched PAADVB prepared (retention time 57.45 min) was estimated to have a M_n of 1,480 Da, a M_w of 1,540 Da and a PDI(M_w/M_n) of 1.0.[I] Figure 3.6 shows the molecular weight distributions of branched PAADVB from GPC. As determined by GPC, the branched PAADVB sample appears relatively monodisperse. The negative peak was derived from the effects of GPC eluent and was not counted in the as molecular weight distribution.[5]

3.2.2 Characterization of materials

3.2.2.1 TGA

The thermochemical and physical properties of MCF and the organic loading in the composite adsorbents were assessed by TGA. For the bare MCF material after template removal through calcination, thermogravimetric analysis showed a negligible

mass loss of 1.0% attributable to a small amount of silanol condensation. This small mass loss has a negligible effect on subsequent thermogravimetric analyses of the polymer loaded mesoporous materials that are used to assess the organic loadings in the composites. For example, the TGA weight loss curves of various PAADVB-loaded MCF samples are shown in Figure 3.7. The PAADVB-loaded MCF samples displayed a mass loss of about 10% over the 27°C to 160°C range. This can be attributed to desorption of adsorbed moisture. No obvious mass loss occurred from 160-220°C. The PAADVB in MCF began to decompose above 220°C in all samples. At about740°C, the PAADVB was completely decomposed and the polymer appeared fully removed as volatile species. These results indicate the maximum stability temperature of these samples under these conditions is about 220°C. Other samples were measured in a similar manner.

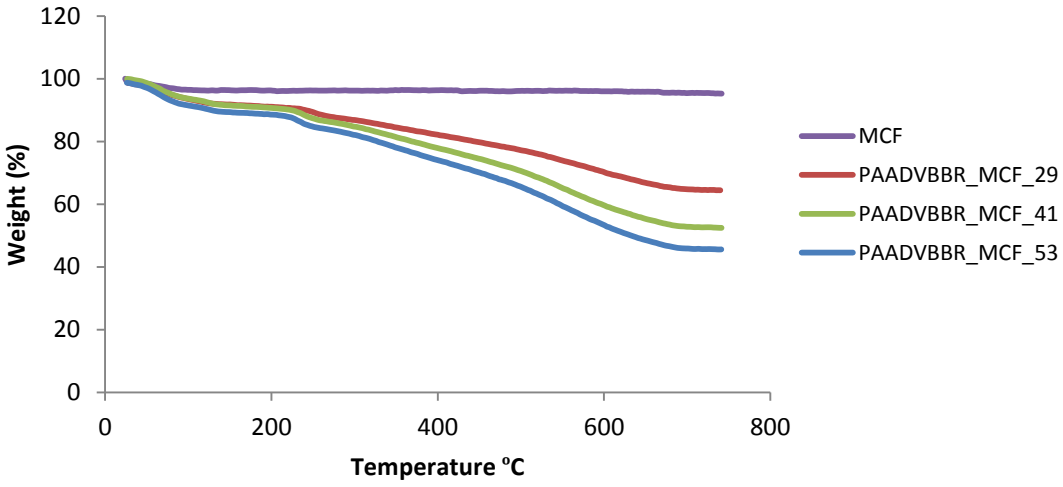

Figure 3.7. TGA profiles of PAADVB-loaded MCF samples of different polymer loadings.

3.2.2.2 Nitrogen adsorption/desorption

The surface area, cell diameter, window and pore volume of MCF and the amine polymer-loaded MCF samples were investigated by nitrogen adsorption/desorption

isotherms. The textural properties of MCF and all the composite samples prepared in this work are presented in Fig 3.8-3.9 and are summarized in Table 3.2. As can be seen, all samples exhibit type IV isotherms according to the IUPAC classification. The isotherms demonstrate a significant reduction in total pore volume and surface area in the composites containing different polymer percentages. The BET surface area, cell diameter, and window and pore volumes of the bare MCF are 660 m^2/g, 39 nm, 17 nm and 2.7 cm^3/g, respectively. The surface area and pore volume of the composites decrease significantly with increasing polymer loadings.[6] The polymer may be largely contained within the pores, although some part of it could also be outside the pores, on the external surface.[7] Together with the TGA results, the data confirm that the amine polymers are loaded into the pore channels of MCF support to a large extent.

Table 3.1. Textural properties of MCF materials before and after polymer loading.

Sample ID	**Adsorption Pore volume ($cm^3\ g^{-1}$)**	**Desorption Pore volume ($cm^3\ g^{-1}$)**	**BET surface area ($cm^2 g^{-1}$)**
MCF	2.7	2.7	660
PAAEPCL_MCF_20	1.9	1.9	334
PAAEPICL_MCF_27	1.4	1.4	235
PAAEPICL_MCF_34	1.1	1.1	173
PAADVBBR_MCF_29	1.3	1.3	255
PAADVBBR_MCF_41	0.8	0.8	150
PAADVBBR_MCF_53	0.5	0.5	80

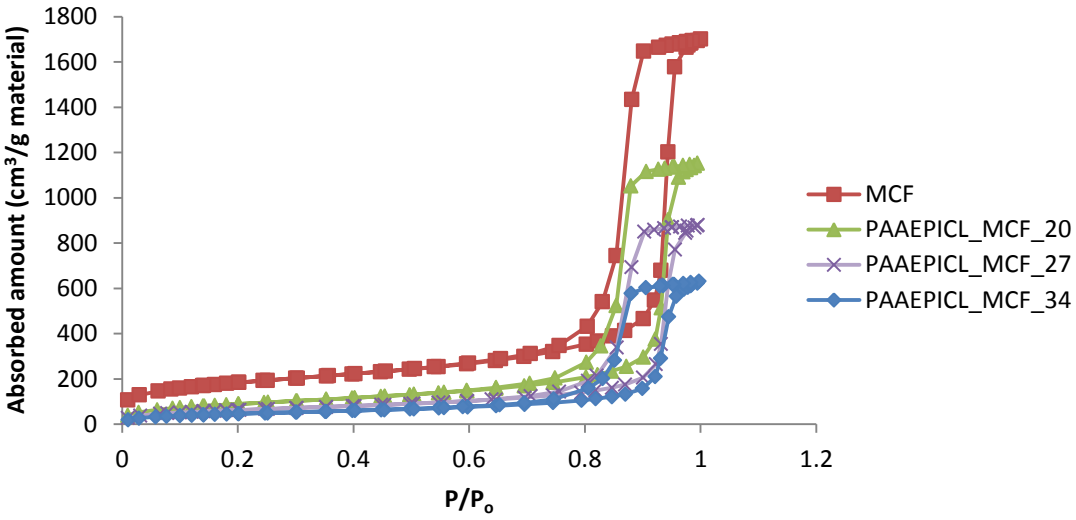

(A)

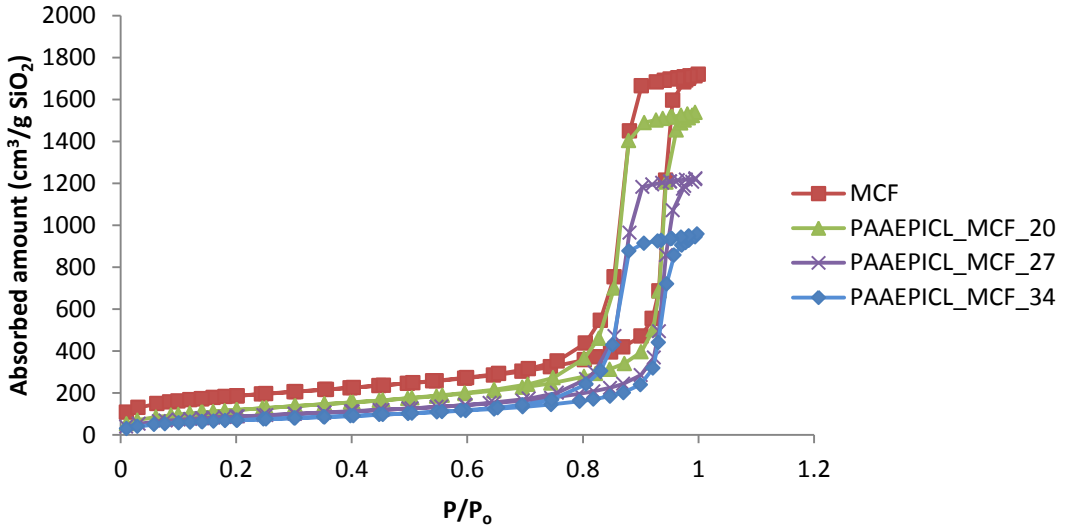

(B)

Figure 3.8. Nitrogen adsorption/desorption isotherms at 77K of samples loaded with cross-linked PAAEPI. (A) Absorbed amount plotted based on mass of material, (B) Absorbed amount plotted based on mass of silica.

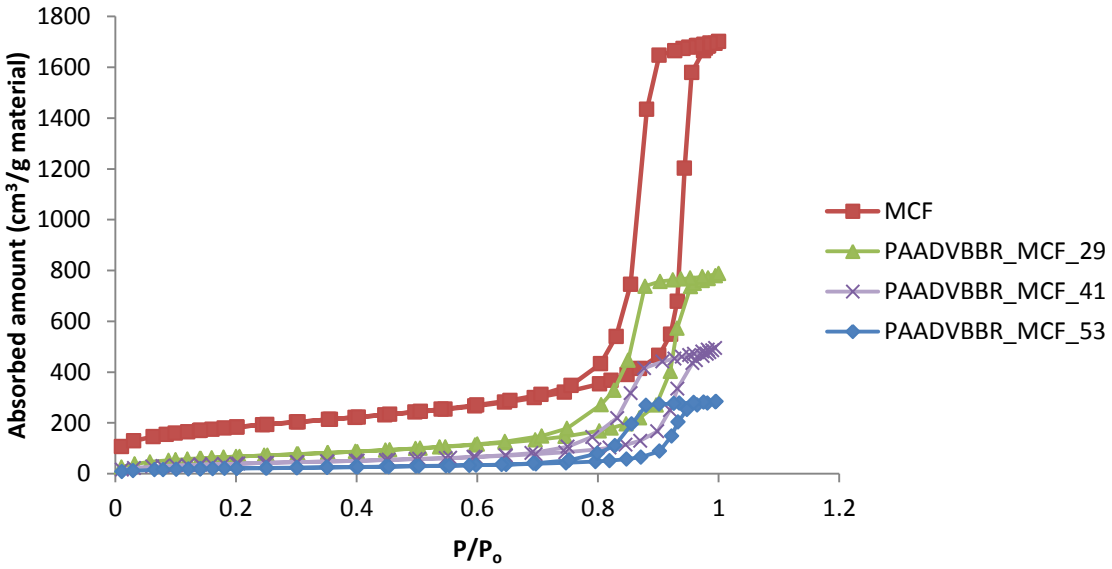

(A)

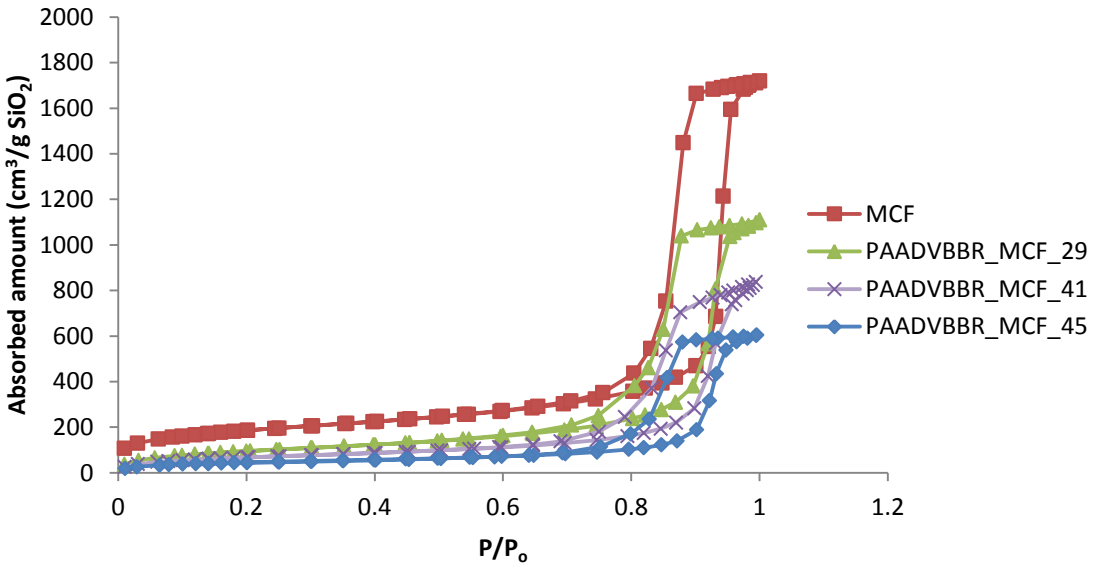

(B)

Figure 3.9. Nitrogen adsorption/desorption isotherms at 77K of samples loaded with branched PAADVB. (A) Absorbed amount plotted based on mass of material, (B) Absorbed amount plotted based on mass of silica.

3.2.2.3 CO_2 adsorption

The maximum theoretical amine efficiency for CO_2 capture under dry conditions at 10%CO_2 concentration (flue gas conditions) and 400ppm concentration (air capture conditions) for the linear PAA, which contains all primary amines, is 0.50. The

calculation of the maximum theoretical amine efficiency for cross-linked PAAEPI is based on the peak integrations in the 400MHz ^{1}H NMR spectra in a 19:1 ratio of (-CH_2 at 2.65ppm):(-CHO at 3.85ppm). At 10% and 400ppm CO_2, the maximum theoretical amine efficiencies are 0.50 (100% primary and secondary amines) and 0.475 (95% primary amines), respectively. The calculation of the maximum theoretical amine efficiency for branched PAADVB is based on the peak integrations in the 400MHz ^{1}H NMR spectra in a 1:70 ratio of (-CH_2 at 2.79 ppm):(Ar at 7.52ppm). For branched PAADVB, which contains only primary amines, the maximum theoretical amine efficiencies are 0.50 for both CO_2 concentrations.

Figure 3.10 presents a comparison of the CO_2 capture performance using 10% CO_2 over linear PAA, cross-linked PAAEPI, and branched PAADVB loaded MCF materials with different polymer loadings. CO_2 adsorption capacity increased for the cross-linked PAAEPI, and branched PAADVB samples as the amine polymers loadings increased. In contrast, CO_2 adsorption capacity decreased with amine loading increase was observed for linear PAA, likely due to the linear nature of the polymer, which inhibited it being effectively loaded into the silica pores. In addition, the linear chains may have also contributed to non-productive, entangled chains inside[8,9,10] the pores of the support, hindering accessibility of CO_2 molecules. By altering the structure of linear to cross-linked, branched and guanidinylated PAA, these new samples may provide higher accessible amine content, allowing for larger CO_2 capacities with the almost linear relationship between capacity and polymer loading, suggesting that the amines are largely accessible in these composite samples. The porosity data presented in Table 3.1 and Figures 3.8-3.9 are consistent with this supposition. It is noteworthy that the cross-linked

PAAEPI yielded higher adsorption capacities than that of the linear PAA and branched PAADVB.

The CO_2 adsorption capacity of cross-linked PAAEPI is higher than that of linear PAA and branched PAADVB at the same loading. For cross-linked PAAEPI, CO_2 sorption capacities of 1.65 and 1.76 mmol CO_2/g sorbent were measured for 27 and 34wt% loading samples, respectively. At the same loading, CO_2 sorption capacities of linear PAA were 1.40 and 1.55 mmol CO_2/g sorbent and for branched PAADVB samples were 1.05 and 1.20 mmol CO_2/g sorbent, respectively (Figure 3.10). In addition, the amine efficiencies of cross-linked PAAEPI, linear PAA and branched PAADVB correspond to their CO_2 adsorption capacity. As can be seen, amine efficiency of cross-linked PAAEPI at 27 and 34 wt% loadings were 0.34 and 0.35, respectively. Meanwhile, at the same loading, amine efficiencies of linear PAA were 0.23 and 0.22, respectively and for branched PAADVB were about 0.23 and 0.21, respectively (Figure 3.11 and Table 3.2). These results could be explained in the hypothesis that the structure of the cross-linked PAAEPI is more open, perhaps having more flexible chains and a lower degree of entanglement, allowing more amine sites to react with CO_2 molecules.[1,8,9] In addition, the presence of the hydroxyl groups (OH) of epichlorohydrin could possibly facilitate amine sites to enhance the capability of CO_2 capture. The hydroxyl groups could influence the chemical adsorption in the hypothesis that there are may change the adsorption mechanism and the carbamates further react with CO_2 to form bicarbonates or carbamate-type zwitterions. Therefore one mole of the amine may react with one mole of CO_2, leading to enhanced adsorption capacity and amine efficiency. Under the conditions used in this work, degree of cross-linking of PAAEPI gave a ratio of 19 repeating PAA

units per one unit of EPI. Thus, the hydroxyl groups may serve to stabilize carbamate type zwitterions, and a mixture of the two adsorption mechanisms may be important (some carbamate formation and some zwitterions stabilization).[11,12]

Table 3.2. Capacity and amine efficiency in 10% CO_2 of the synthesized adsorbent samples.

Sample ID	Amine loading (mmol N/g)	Capacity (mmol CO_2/g sorbent)	Amine efficiency (mmol CO_2/mmol N)
PAALN_MCF_32	5.74	1.35	0.24
PAALN_MCF_41	7.24	1.56	0.22
PAALN_MCF_54	9.51	1.36	0.14
PAAEPICL_MCF_20	3.49	0.98	0.28
PAAEPICL_MCF_27	4.73	1.65	0.35
PAAEPICL_MCF_34	5.20	1.76	0.34
PAADVBBR_MCF_29	4.93	1.11	0.23
PAADVBBR_MCF_41	6.97	1.27	0.18
PAADVBBR_MCF_53	9.00	1.34	0.15

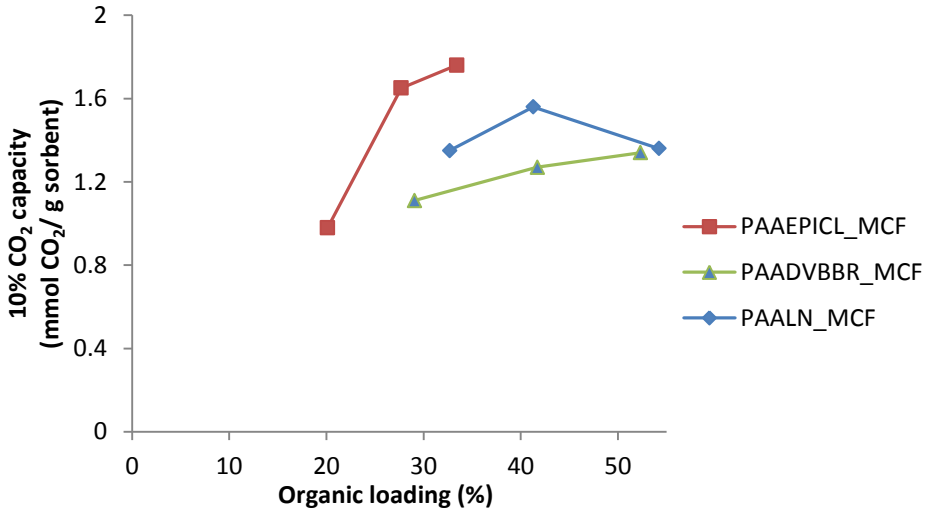

Figure 3.10. CO_2 sorption performances of linear PAA, cross-linked PAAEPI, and branched PAADVB loaded at different organic loadings in 10% CO_2.

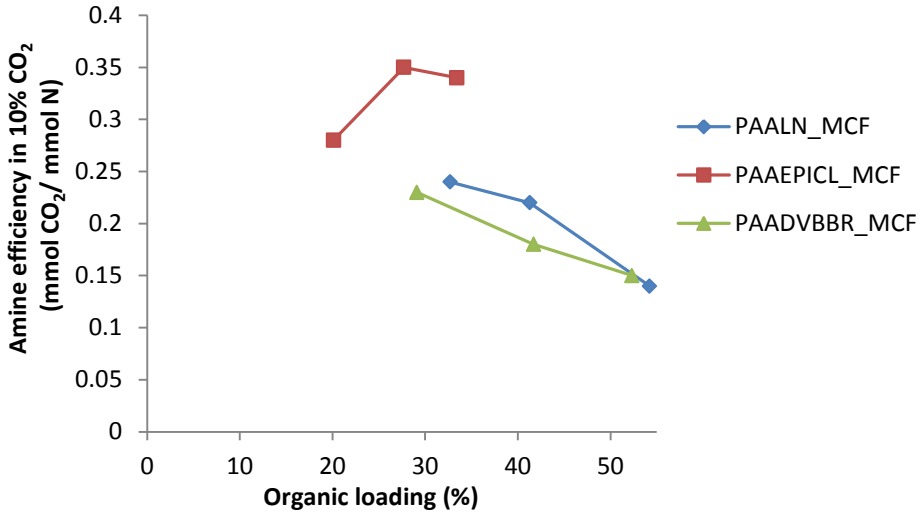

Figure 3.11. Amine efficiency of linear PAA, cross-linked PAAEPI, and branched PAADVB at different organic loadings at 10% CO_2 conditions.

Figure 3.12 presents a comparison of the CO_2 capture performance using a 400 ppm CO_2 gas streams as a function of the polymer type (linear PAA, cross-linked PAAEPI, and branched PAADVB) loading in the MCF support. CO_2 adsorption capacity of linear PAA, cross-linked PAAEPI, and branched PAADVB behave similar trends, increasing with loading, then yielding an insignificant change at higher loadings. However, in comparison at the same loading (29wt%) of linear PAA, cross-linked PAAEPI and branched PAADVB, CO_2 adsorption capacity of cross-linked PAAEPI (0.82 mmol CO_2/g sorbent) yielding higher than that of linear PAA (0.70 mmol CO_2/g sorbent) and branched PAADVB (0.61 mmol CO_2/g sorbent). The amine efficiency of these amine polymers correspond to their CO_2 adsorption capacity. The amine efficiency of linear PAA, cross-linked PAAEPI and branched PAADVB at 29 wt% loading were 0.11, 0.17 and 0.12, respectively (Figure 3.13, Table 3.3). The CO_2 adsorption performance of

cross-linked PAAEPI in 400 ppm is consistent with 10% CO_2 with the same hypothesis as discuss above.

Table 3.3. Capacity and amine efficiency in 400 ppm CO_2 of the synthesized adsorbent samples.

Sample ID	Amine loading (mmol N/g)	Capacity (mmol CO_2/g sorbent)	Amine efficiency (mmol CO_2/mmol N)
PAALN_MCF_32	5.74	0.63	0.11
PAALN_MCF_41	7.24	0.86	0.12
PAALN_MCF_54	9.51	0.84	0.09
PAAEPICL_MCF_20	3.49	0.47	0.13
PAAEPICL_MCF_27	4.73	0.85	0.18
PAAEPICL_MCF_34	5.20	0.83	0.16
PAADVBBR_MCF_29	4.93	0.61	0.12
PAADVBBR_MCF_41	6.97	0.76	0.11
PAADVBBR_MCF_53	9.00	0.77	0.09

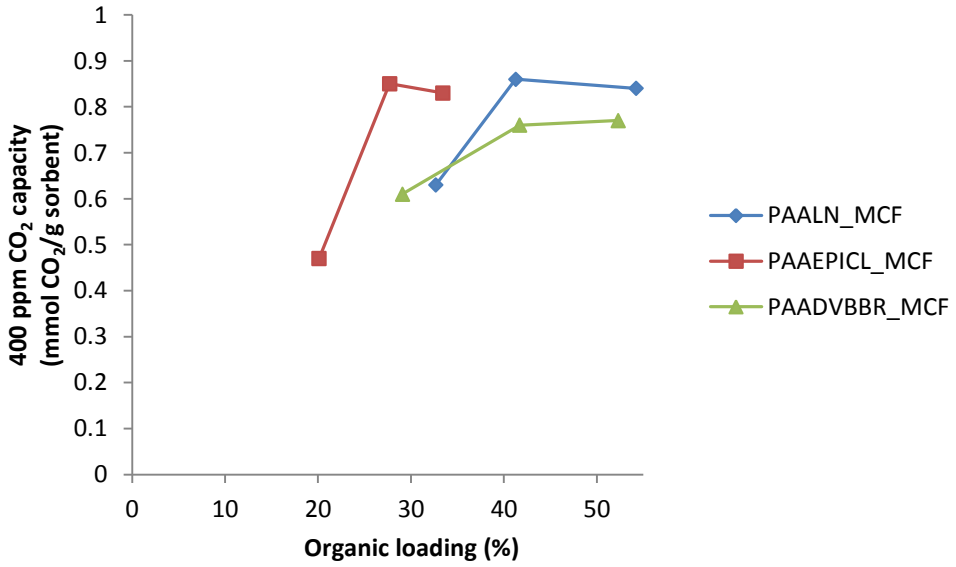

Figure 3.12. CO_2 sorption performances of linear PAA, cross-linked PAAEPI, and branched PAADVB loaded at different organic loadings in 400 ppm.

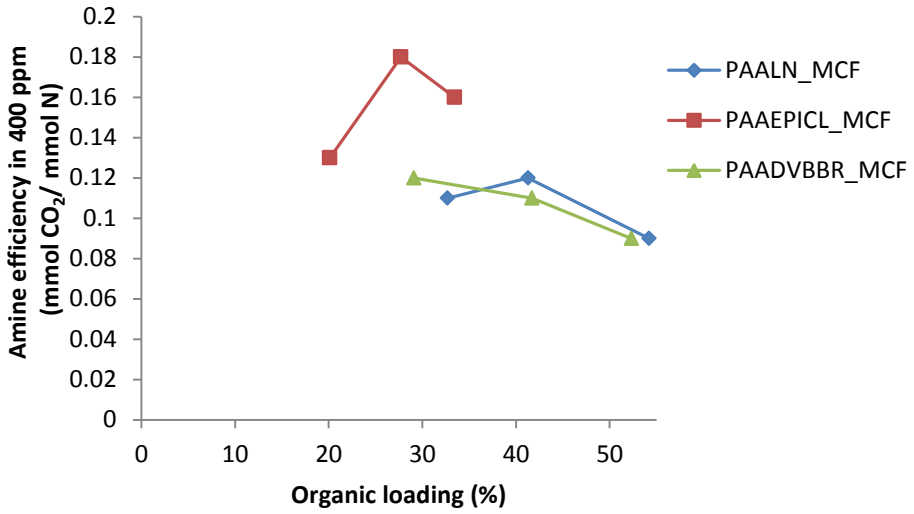

Figure 3.13. Amine efficiency of linear PAA, cross-linked PAAEPI, and branched PAADVB at different organic loadings at 400 ppm conditions.

3.4 Conclusions

A polymer rich in primary amines, specifically linear poly(allylamine), was altered to cross-linked and branched. Cross-linked PAAEPI and branched PAADVB were synthesized and characterized. Subsequently, class 1 materials were prepared for CO_2 capture by wet-impregnation porous mesoporous silica foams using cross-linked PAAEPI and branched PAADVB. The CO_2 adsorption performances were investigated under moderately dilute and ultra-dilute gas streams compared with linear PAA. The results suggest that altering the linear polymer chains of PAA by using epichlorohydrin as a cross-linking agent is a promising way to give materials that bind CO_2 more efficiently in both moderately dilute gas streams and ultra-dilute gas streams conditions.

3.5 References

1 Peacock, A.; Calhoun, A. *Polymer Chemistry*. Hanser Gardner Publications. Cincinnati, 2006.

2 Gillespie, T. The Use of Viscosity Data to Assess Molecular Entanglement in Dilute Polymer Solutions. *J. Polym. Sci: Part C.***1963,** 3, 31.

3 Lukens, W.; Schmidt-Winkel,P.; Zhao, DY.; Feng, JL.; Stucky,GD. Evaluating Pore Sizes in Mesoporous Materials: A Simplified Standard Adsorption Method and a Simplified Broekhoff−de Boer Method. *Langmuir* **1999**, 15, 5403.

4 Lindfors, K.B.; Pan, S.; Dreyfuss, P. Two-Dimentional NMR Determination of the Regiosequence Distribution in Polyepichlorohydrin. *Macromolecules* **1993**, 26, 2919.

5 Thomson Instrument Company. Measurement of Molecular Weight Distribution of Poly(Allylamine)Hydrochloride.http://www.hplc.com/Shodex/english/dc062001.htm.

6 Xu, X.; Song, C.; Miller, B.G, Scaroni, A.W. Adsorption separation of carbon dioxide from flue gas of natural gas-fired boiler by a novel nanoporous "molecular basket" adsorbent. *Fuel Processing Technol.* **2005**, 86, 1457.

7 Xu,X.;Novochinskii,I.; Song, C.S. Low-Temperature Removal of H_2S by Nanoporous Composite of Polymer-Mesoporous Molecular Sieve MCM-41 as Adsorbent for Fuel Cell Applications. *Energy Fuels* **2005**, 19, 2214.

8 Aharoni, S.M. Segmental Interpenetrations and Entanglements. *J. Polym. Sci. Polym Lett Ed.* **1974**, 12, 549.

9 Choi, S.H.; Jansen, J.C.; Tasselli, F.; Barbieri, G.; Drioli, E. In-line formation of chemically cross-linked P84® co-polyimide hollow fibre membranes for H_2/CO_2 separation. *Sep. Purif. Technol.* **2010**, 76(2), 132.

10 Mcleish, T.B.C. Tube theory of entangled polymer dynamics. *Advances in Physics* **2002**, 51(6), 1379.

11 Yue, M.B.; Chun, Y.; Cao, Y.; Dong, X.; Zhu, J. CO_2 Capture by As-prepared SBA -15 with an Occluded Organic Template. *Adv. Funct. Mater.* **2006**, 16, 1717.

12 Delaney, W., Knowles, G.; Chaffee, A. Hybrid Mesopous Materials for Carbon Dioxide Separation. *Prepr. Am. Chem. Soc., Div. Fuel Chem*. **2002**, 47, 65.

CHAPTER 4

SUMMARY AND FUTURE WORK

4.1 Summary

The major goals of this thesis are (1) to synthesize and characterize polymers that are rich in primary amines. (2) create class 1 adsorbents using these polymers, by impregnating the polymers into the pore space of a large pore mesocellular foam silica, and (3) to evaluate the CO_2 adsorption capacities of the new polymeric amine – silica composite materials under simulated air capture and flue gas capture conditions and (4) to assess the impact of cross-linking and branching polymer structure on the CO_2 adsorption properties.

Polymers rich in primary amines, specifically poly(vinylamine)(PVAm), poly (allylamine)(PAA), cross-linked poly(allylamine) using epichlorohydrin (PAAEPI), and branched poly(allylamine) using divinylbenzene (PAADVB) were synthesized and characterized. Under the conditions used in this work, PVAm had a high molecular weight that was likely too large for preparation of effective class 1 CO_2 adsorbent materials. In contrast, PAA and their derivatives yielded low molecular weights and were prepared as class 1 material for CO_2 capture by impregnating porous mesocellular silica foams (MCF) with the polymers. The CO_2 adsorption performance of the composites were investigated under moderately dilute gas streams (10% CO_2 concentration or flue gas conditions), and ultra-dilute gas streams (400 ppm CO_2 concentration or air capture conditions).

The CO_2 adsorption performance of PAA composite materials were compared with materials made branched PEI and linear PEI, with the materials made from branched

PEI representing the best materials currently known for air capture. The results indicate that PAA is a promising candidate for CO_2 capture, especially in ultra-dilute gas streams such as ambient air, which is requires an extremely efficient adsorbent tuned to bind CO_2 very strongly. However, the linear nature of the polymer precludes its effective use at high polymer loadings, as the polymer cannot be effectively loaded into the silica pores. In addition, the linear chains may have also contributed to non-productive, entangled chains inside the pores of the support, hindering accessibility of CO_2 molecules.

Cross-linked PAAEPI and branched PAADVB were proposed to improve the macromolecular structure and improve the CO_2 adsorption performance achieved with linear PAA. The results suggest that cross-linked PAAEPI was a promising candidate to improve the amine efficiency of PAA for both flue gas and air capture conditions. The summary of CO_2 adsorption capacity and amine efficiency of amine polymers that were prepared as class 1 materials and studied in this work are presented in Figure 4.1-4.4.

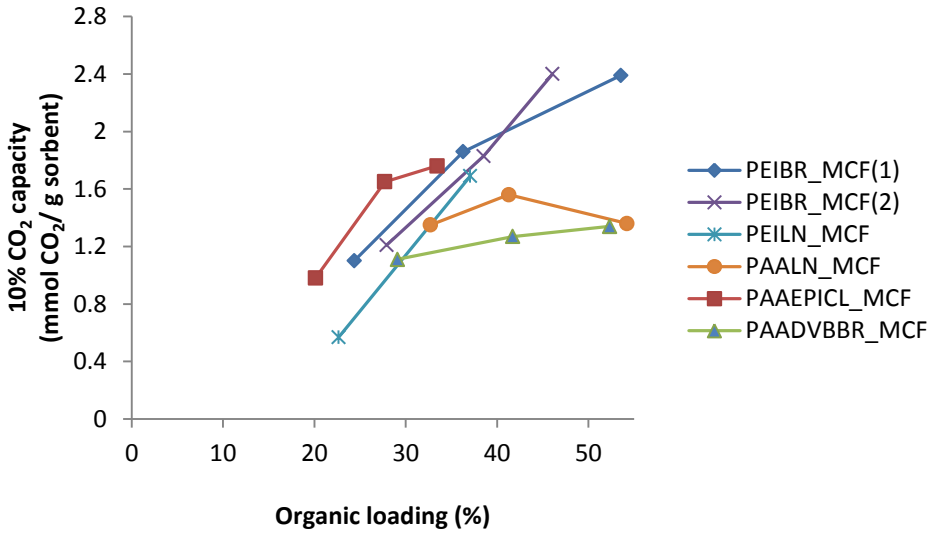

Figure 4.1. Summary of CO_2 adsorption capacities of branched PEI, linear PEI, linear PAA, cross-linked PAAEPI, and branched PAADVB in 10% CO_2.

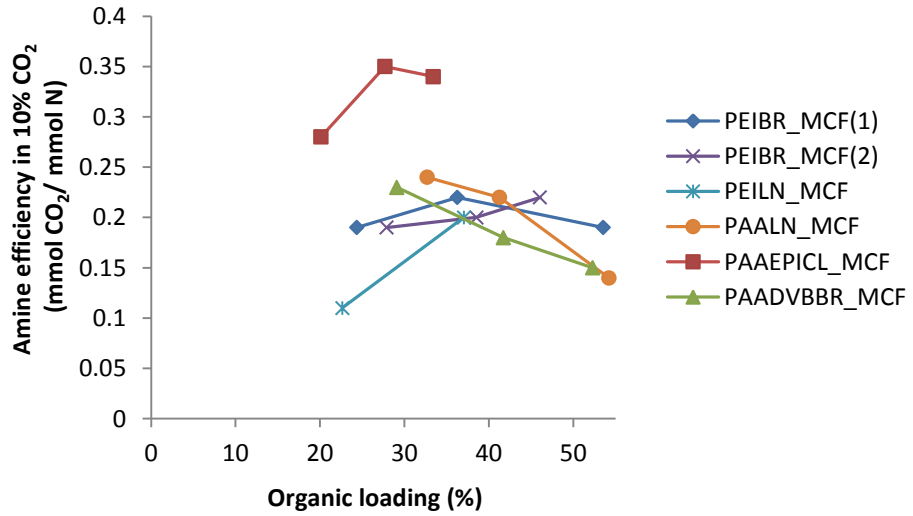

Figure 4.2. Summary of amine efficiency of branched PEI, linear PEI, linear PAA, cross-linked PAAEPI, and branched PAADVB in 10% CO_2.

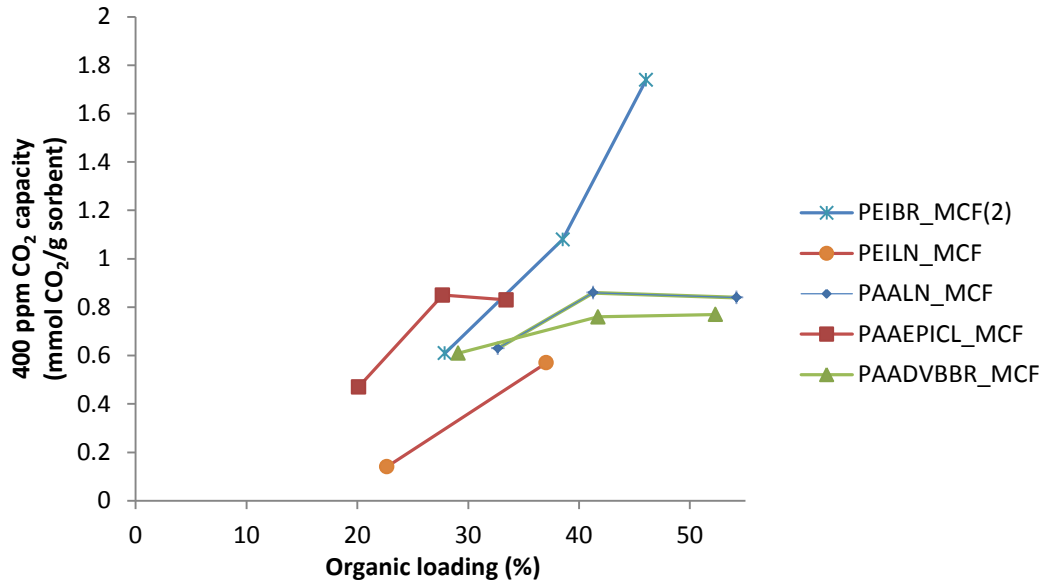

Figure 4.3. Summary of CO_2 adsorption capacities of branched PEI, linear PEI, linear PAA, cross-linked PAAEPI, and branched PAADVB in 400 ppm.

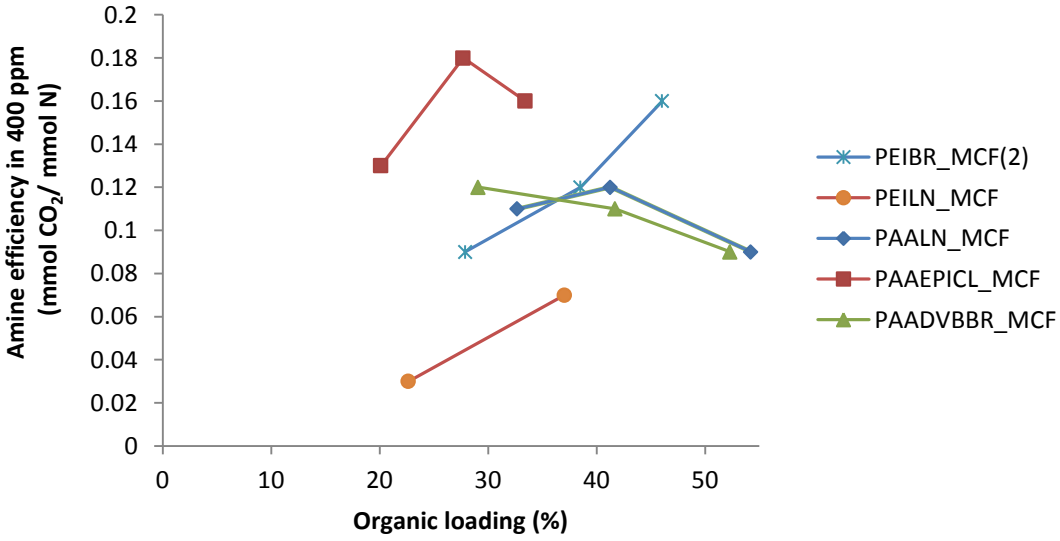

Figure 4.4. Summary of amine efficiency of branched PEI, linear PEI, linear PAA, cross-linked PAAEPI, and branched PAADVB in 400 ppm.

4.2 Reccomendations for future work

1) For class 1 materials, low molecular weight and highly branched amine polymer should be consider as to the most suitable candidates for impregnation into the pores of silica supports because of short chain and compact structure. Moreover, highly branched polymers are suggested here to adopt a lower degree of entanglement, leading to favorable accessibility of amine sites for interaction with CO_2 molecules.

2) Perfectly branched poly(allylamine) such as dendrimer structure is highly recommended for CO_2 capture, especially in ultra-dilute gas streams such as ambient air.

3) Silica supports with larger pore volume are recommended for class 1 material because of the larger amount of amine groups can be loaded into the pores.